

Lactic acid production from glucose by using divalent transition metal oxide catalyst
on magnesium oxide support without alkaline solution



A Thesis Submitted in Partial Fulfillment of the Requirements
for the Degree of Master of Engineering in Chemical Engineering

Department of Chemical Engineering

Faculty of Engineering

Chulalongkorn University

Academic Year 2018

Copyright of Chulalongkorn University

การผลิตกรดแลคติกจากกลูโคสโดยใช้ตัวเร่งปฏิกิริยาโลหะทรานซิชันออกไซด์ที่มีเลขสถานะ
ออกซิเดชันเท่ากับสอง บนตัวรองรับแมกนีเซียมออกไซด์ โดยไม่ใช้สารละลายเบส



วิทยานิพนธ์นี้เป็นส่วนหนึ่งของการศึกษาตามหลักสูตรปริญญาวิทยาศาสตรมหาบัณฑิต
สาขาวิชาวิศวกรรมเคมี ภาควิชาวิศวกรรมเคมี
คณะวิศวกรรมศาสตร์ จุฬาลงกรณ์มหาวิทยาลัย
ปีการศึกษา 2561
ลิขสิทธิ์ของจุฬาลงกรณ์มหาวิทยาลัย

Thesis Title	Lactic acid production from glucose by using divalent transition metal oxide catalyst on magnesium oxide support without alkaline solution
By	Miss Tanyatorn Udomcharoensab
Field of Study	Chemical Engineering
Thesis Advisor	Professor PIYASAN PRASERTHDAM, Dr.Ing.
Thesis Co Advisor	Wipark Anutrasakda, Ph.D.

Accepted by the Faculty of Engineering, Chulalongkorn University in Partial Fulfillment of the Requirement for the Master of Engineering

..... Dean of the Faculty of Engineering
(Professor SUPOT TEACHAVORASINSKUN, D.Eng.)

THESIS COMMITTEE

..... Chairman
(Associate Professor Kasidit Nootong, Ph.D.)

..... Thesis Advisor
(Professor PIYASAN PRASERTHDAM, Dr.Ing.)

..... Thesis Co-Advisor
(Wipark Anutrasakda, Ph.D.)

..... Examiner
(Rungthiwa Methaapanon, Ph.D.)

..... External Examiner
(Nilubon Jonganurakkun, Ph.D.)

ฉันทยธรรม์ อุดมเจริญทรัพย์ : การผลิตกรดแลคติกจากกลูโคสโดยใช้ตัวเร่งปฏิกิริยาโลหะ
 ทรานซิซันออกไซด์ที่มีเลขสถานะออกซิเดชันเท่ากับสอง บนตัวรองรับแมกนีเซียม
 ออกไซด์ โดยไม่ใช้สารละลายเบส. (Lactic acid production from glucose by
 using divalent transition metal oxide catalyst on magnesium oxide support
 without alkaline solution) อ.ที่ปรึกษาหลัก : ศ. ดร.ปิยะสาร ประเสริฐธรรม, อ.ที่
 ปรึกษาร่วม : อ. ดร.วิภาค อนุตรศักดิ์ดา

งานวิจัยนี้ศึกษาผลกระทบจากชนิดของตัวเร่งปฏิกิริยาที่มีโลหะทรานซิซันออกไซด์ที่มี
 เลขสถานะออกซิเดชันเท่ากับสอง บนตัวรองรับแมกนีเซียมออกไซด์ ต่อปริมาณการผลิตกรด
 คติคจากกลูโคส โดยชนิดของโลหะได้แก่ คอปเปอร์, โคบอลต์, นิกเกิล และ สังกะสี เติมโลหะด้วย
 ปริมาณ 1.5, 5 และ 10 มิลลิโมลต่อกรัมของตัวเร่งปฏิกิริยา ตัวเร่งปฏิกิริยามีการเติมด้วยดีคาเฮ
 คือ เฮกซะเดซิลไตรเมทิลแอมโมเนียม โบรไมด์ (CTAB) ทำปฏิกิริยาภายใต้สภาวะที่ไม่มีการเติม
 สารละลายเบสเพื่อลดอัตราการกัดกร่อนต่อเครื่องปฏิกรณ์และลดผลกระทบต่อสิ่งแวดล้อม ตัวเร่ง
 ปฏิกิริยาสังเคราะห์ด้วยวิธีไฮโดรเทอร์มอล และวิเคราะห์ด้วยเทคนิคต่างๆ จากผลการวิเคราะห์
 ด้วยเทคนิคการเลี้ยวเบนรังสีเอกซ์ (XRD) พบสถานะของโลหะที่ถูกรีดิวซ์ของตัวเร่งปฏิกิริยาที่ใช้แล้วใน
 ตัวเร่งปฏิกิริยา คอปเปอร์-CTAB บนแมกนีเซียมออกไซด์ และ โคบอลต์-CTAB บนแมกนีเซียม
 ออกไซด์ แสดงให้เห็นว่ามีการใช้อะตอมออกซิเจนจากโลหะออกไซด์ในการทำปฏิกิริยา ในขณะที่
 ตัวเร่งปฏิกิริยาที่ใช้แล้วในนิกเกิล-CTAB บนแมกนีเซียมออกไซด์ และสังกะสี-CTAB บนแมกนีเซียม
 ออกไซด์ แสดงสถานะของโลหะไฮดรอกไซด์ ซึ่งคาดว่าเกิดจากการดูดซับทางเคมีของโมเลกุลน้ำที่
 ผิวของตัวเร่งปฏิกิริยา ปริมาณการเปลี่ยนแปลงของกลูโคสสัมพันธ์กับปริมาณของโลหะที่หลุด
 ออกมาจากตัวเร่งปฏิกิริยา แสดงให้เห็นว่าไอออนของโลหะและความเป็นเบสในสารละลายมี
 ผลกระทบต่อการเปลี่ยนแปลงของกลูโคสมาก ในขณะที่ปริมาณการเลือกเกิดของกรดแลคติก
 สอดคล้องกับความเป็นเบสจากผลการไตเตรตตัวเร่งปฏิกิริยาด้วยกรด แสดงให้เห็นว่าความเป็นเบส
 ที่ผิวของตัวเร่งปฏิกิริยามีผลกระทบต่อการเลือกเกิดของกรดแลคติกมาก

สาขาวิชา วิศวกรรมเคมี

ปีการศึกษา 2561

ลายมือชื่อนิสิต

ลายมือชื่อ อ.ที่ปรึกษาหลัก

ลายมือชื่อ อ.ที่ปรึกษาร่วม

5970441821 : MAJOR CHEMICAL ENGINEERING

KEYWORD: lactic acid, glucose, magnesium oxide, transition metal oxide

Tanyatorn Udomcharoensab : Lactic acid production from glucose by using divalent transition metal oxide catalyst on magnesium oxide support without alkaline solution. Advisor: Prof. PIYASAN PRASERTHDAM, Dr.Ing. Co-advisor: Wipark Anutrasakda, Ph.D.

This research was studied the effects of the type of divalent metal oxide (Cu, Co, Ni, and Zn) supported on magnesium oxide catalyst using the hexadecyltrimethylammonium bromide (CTAB) as the capping agent with metal loading at 1.5, 5, and 10 mmol/gram-catalyst on lactic acid production from glucose. To achieve the lactic acid production of lower reactor corrosion rate and being environmentally friendly, the reaction was performed in an alkali additive-free environment. The catalysts were synthesized by hydrothermal method and characterized by various techniques. The XRD pattern of spent CuCTAB/MgO and CoCTAB/MgO catalyst showed the reduced metal species indicated the used of oxygen atom from metal oxide for the reaction. While the NiCTAB/MgO and ZnCTAB/MgO showed peak of metal hydroxide in spent catalyst which suggested that the chemisorption of water molecule at the catalyst surface has been occurred. The glucose conversion from various catalysts were related to the amount of metal leaching from the ICP result, which indicated that the metal ion and basicity from metal hydroxide in the solution has very effected to the glucose conversion. While, the selectivity of lactic acid was consistent with basicity from acid titration suggested that the basicity of catalyst surface has an important role to the selectivity of lactic acid.

Field of Study: Chemical Engineering

Student's Signature

Academic Year: 2018

Advisor's Signature

Co-advisor's Signature

ACKNOWLEDGEMENTS

This thesis becomes a reality with the many kind supports. I would like to extend my sincere thanks to all of them.

I cannot express enough thanks to my advisor, Professor Dr. Piyasan Praserttham and my co-advisor, Dr. Wipark Anutrasakda for the valuable suggestion, useful discussion, very supporting and many knowledge for this research. All guidance helped me throughout the duration of research.

I would also be grateful to Associate Professor Kasidit Nootong, as the chairman, Dr. Rungthiwa Methaapanon and Dr. Nilubon Jong-Anurakkun as the members of the thesis committee for their comment and good advice.

Furthermore, I would like to gratefully thank Global Green Chemicals Public Company Limited (GGC) for the financial support. And thanks my beloved friends and the scientist of Center of Excellence on Catalysis and Catalytic Reaction Engineering, Chulalongkorn University for the supports and encouragements.

Finally, I would like to thank to my beloved parents, who have always been the source of motivation, support and encouragement through the time spent on study.

จุฬาลงกรณ์มหาวิทยาลัย
CHULALONGKORN UNIVERSITY

Tanyatorn Udomcharoensab

TABLE OF CONTENTS

	Page
ABSTRACT (THAI).....	iii
ABSTRACT (ENGLISH).....	iv
ACKNOWLEDGEMENTS.....	v
TABLE OF CONTENTS.....	vi
LIST OF TABLES.....	x
LIST OF FIGURES.....	xi
LIST OF SCHEMES.....	xiii
CHAPTER I INTRODUCTION.....	14
1.1 Introduction.....	14
1.2 Objective.....	17
1.3 The scopes of research.....	17
1.4 Research methodology.....	19
CHAPTER II THEORY AND LITERATURE REVIEWS.....	20
2.1 Lactic acid.....	20
2.1.1 Structure and properties of the lactic acid.....	20
2.1.2 Applications of lactic acid.....	21
2.1.3 The synthesis of lactic acid.....	23
2.2 The chemocatalytic conversion of glucose into lactic acid.....	24
2.2.1 Hydrothermal method.....	24
2.2.1.1 Hydrothermal methods with an alkaline solution.....	25

2.2.1.2 Hydrothermal methods with heterogeneous catalyst and alkaline solution.....	25
2.2.1.3 Hydrothermal methods with heterogeneous catalyst (without alkaline solution).....	27
2.2.2 The reaction under mild conditions.....	29
2.2.2.1 The reaction under mild conditions by using an alkaline solution.....	29
2.2.2.2 The reaction under mild conditions by using heterogeneous catalyst and alkaline solution.....	30
2.2.2.3 The reaction under mild conditions by using a heterogeneous catalyst (without alkaline solution).....	32
2.3 The important reaction in a base-catalyzed lactic acid production.....	33
2.3.1 Isomerization reaction.....	33
2.3.2 The retro-aldol reaction.....	33
CHAPTER III EXPERIMENTAL.....	35
3.1 Materials and chemicals.....	35
3.2 Catalyst preparation.....	36
3.3 Catalytic reaction procedure.....	36
3.4 Product analysis.....	37
3.5 Catalyst characterization.....	37
3.5.1 X-ray diffraction (XRD).....	37
3.5.2 Scan electron microscope (SEM) and energy x-ray spectroscopy (EDX) ...	38
3.5.3 N ₂ -physisorption.....	38
3.5.4 H ₂ temperature programmed reduction (H ₂ -TPR).....	38
3.5.5 CO ₂ temperature programmed desorption (CO ₂ -TPD).....	38

3.5.6 Acid titration	39
3.5.7 Inductively Coupled Plasma-Atomic Emission Spectroscopy (ICP-AES)	39
CHAPTER IV RESULTS AND DISCUSSION	40
4.1 Effects of the type of divalent metal oxide supported on MgO catalysts on the lactic acid production from glucose	40
4.1.1 The physical and chemical properties of catalysts.....	40
4.1.1.1 X-Ray Diffraction (XRD).....	40
4.1.1.2 Scan electron microscope (SEM) and energy x-ray spectroscopy (EDX)	44
4.1.1.3 N ₂ -physisorption	47
4.1.1.4 H ₂ temperature programmed reduction (H ₂ -TPR)	47
4.1.1.5 CO ₂ temperature programmed desorption (CO ₂ -TPD)	49
4.1.1.6 Acid titration.....	50
4.1.1.7 Inductively Coupled Plasma-Atomic Emission Spectroscopy (ICP-AES).....	51
4.1.2 Catalytic performance for lactic acid production from glucose	53
4.2 Effects of the amounts of metal oxide loading on MgO catalysts on the lactic acid production from glucose	57
4.2.1 The physical and chemical properties of catalysts.....	57
4.2.1.1 X-Ray Diffraction (XRD).....	57
4.2.1.2 Acid titration.....	59
4.2.1.3 Inductively Coupled Plasma-Atomic Emission Spectroscopy (ICP-AES).....	60
4.2.2 Catalytic performance for lactic acid production from glucose	60
4.3 Proposed mechanism	63

CHAPTER V CONCLUSIONS AND RECOMMENDATIONS	66
5.1 Conclusions	66
5.2 Recommendations.....	67
REFERENCES	68
APPENDIX.....	74
APPENDIX A CALCULATION OF CATALYST PREPARATION.....	75
APPENDIX B CALCULATION OF TOTAL BASIC SITES OF CATALYST	76
APPENDIX C SEM IMAGES AND EDX MAPS OF METAL OXIDE SUPPORTED ON MgO CATLYST	77
APPENDIX D CALIBRATION CURVES OF REAGENTS.....	81
APPENDIX E THE DEGRADATION OF INTERMEDIATES AND LACTIC ACID TO BY- PRODUCTS.....	85
APPENDIX F SUPPLEMENTARY DATA	86
VITA.....	90

LIST OF TABLES

	Page
Table 2.1 The chemical and physical properties of lactic acid.....	12
Table 3.1 List of the chemical in this research.....	26
Table 4.1 The elemental compositions of various metal loading on MgO catalysts from energy X-ray spectroscopy.....	36
Table 4.2 The specific surface area of the catalysts with metal loading at 1.5 mmol/g-cat.....	38
Table 4.3 Amounts of total basicity of MgO and metal oxide supported on MgO catalysts which calculated from CO ₂ -TPD technique.....	41
Table 4.4 Amounts of basicity of fresh and used MgO and metal oxide supported on MgO catalysts which calculated from acid titration technique.....	42
Table 4.5 Amounts of metal leaching from lactic acid production from glucose.....	43
Table 4.6 Amounts of basicity of fresh various metal loading on MgO catalyst which was calculated from acid titration technique.....	50
Table 4.7 Amounts of metal leaching from lactic acid production from glucose by using catalysts at various metal loading.....	51
Table E.1 Effect of reaction time on lactic acid production from glucose by using ZnCTAB/MgO with metal loading of 1.5 mmol/g-cat.....	76
Table E.2 Textural properties and catalytic activity for lactic acid production from glucose.....	77

LIST OF FIGURES

	Page
Figure 1.1 U.S. lactic acid market volume by application, 2014 - 2025 (Kilo Tons).....	15
Figure 2.1 Lactic acid forms.....	20
Figure 2.2 Global market of lactic acid in 2014.....	22
Figure 2.3 The role of lactic acid for the synthesis of useful chemicals.....	22
Figure 2.4 PLA products.....	23
Figure 2.5 Isomerization of glucose to fructose in alkali.....	33
Figure 2.6 The aldol reaction mechanism.....	34
Figure 4.1 XRD patterns of fresh metal oxide supported on MgO catalysts with metal loading at 1.5 mmol/g-cat.....	41
Figure 4.2 XRD patterns of used metal oxide supported on MgO catalysts with metal loading at 1.5 mmol/g-cat in the lactic acid synthesis from glucose at 140°C for 1 h.....	42
Figure 4.3 SEM images and EDX maps of metal oxide supported on MgO catalysts with metal loading of 1.5 mmol/g-cat.....	46
Figure 4.4 H ₂ -TPR profiles of metal oxide supported on MgO catalysts.....	48
Figure 4.5 CO ₂ -TPD profiles of MgO and metal oxide supported on MgO catalysts....	49
Figure 4.6 Catalytic activity of metal oxide supported on MgO catalysts at the various reaction temperature.....	53
Figure 4.7 Selectivity of lactic acid of metal oxide supported on MgO catalysts at the various reaction temperature.....	54
Figure 4.8 XRD patterns of fresh metal oxide supported on MgO catalysts with metal loading at 5 mmol/g-cat.....	57
Figure 4.9 XRD patterns of used metal oxide supported on MgO catalysts with metal loading at 5 mmol/g-cat in the lactic acid synthesis from glucose at 110°C for 1 h....	58

Figure 4.10 Catalytic activity of various metal loading on MgO catalysts at 110°C.....	61
Figure 4.11 Selectivity of lactic acid of various metal loading on MgO catalysts at 110°C.....	61
Figure 4.12 Catalytic activity of various metal loading on MgO catalyst at 140°C.....	62
Figure 4.13 Selectivity of lactic acid of various metal loading on MgO catalyst at 140°C.....	63
Figure B.1 The calibration curve of carbon dioxide obtained from Micromeritics 2750.....	76
Figure C.1 SEM images at 500 and 6,000 magnification and EDX mapping of O and Mg for CuCTAB/MgO with Cu loading of 1.5 mmol/g-cat.....	77
Figure C.2 SEM images at 500 and 6,000 magnification and EDX mapping of O and Mg for CoCTAB/MgO with Co loading of 1.5 mmol/g-cat.....	78
Figure C.3 SEM images at 500 and 6,000 magnification and EDX mapping of O and Mg for NiCTAB/MgO with Ni loading of 1.5 mmol/g-cat.....	79
Figure C.4 SEM images at 500 and 6,000 magnification and EDX mapping of O and Mg for ZnCTAB/MgO with Zn loading of 1.5 mmol/g-cat.....	80
Figure D.1 Calibration curve of glucose.....	81
Figure D.2 Calibration curve of lactic acid.....	82
Figure D.3 Calibration curve of fructose.....	82
Figure D.4 Calibration curve of glyceraldehyde.....	83
Figure D.5 Calibration curve of formic acid.....	83
Figure D.6 Calibration curve of acetic acid.....	84

LIST OF SCHEMES

	Page
Scheme 2.1 Reaction pathway of production of lactic acid and acetic acid from D-glucose with CuO under alkaline hydrothermal conditions.....	26
Scheme 2.2 Reaction pathway for LaCoO ₃ catalytic conversion of glucose into lactic acid.....	28
Scheme 2.3 Reaction pathway of base-catalyzed the lactic acid production from glucose at room temperature under anaerobic conditions.....	30
Scheme 2.4 The mechanistic pathways for glucose conversion into a lactic acid by using Cu as a catalyst in the present of alkali.....	32
Scheme 4.1 Proposed reaction pathway for the usage of oxygen atom of CuCTAB/MgO catalyst.....	64
Scheme 4.2 Proposed reaction pathway for the usage of oxygen atom of CoCTAB/MgO catalyst.....	65
Scheme 4.3 Proposed reaction pathway for the usage of the hydroxyl group at the catalyst surface of metal oxide supported on MgO catalysts.....	65

CHAPTER I

INTRODUCTION

1.1 Introduction

Over the last decade, the global warming and energy crisis are major problems which must be concerned. The imbalance between the rapid consumption and the slow formation of fossil fuels results in the decrease in the global fossil resources. Moreover, the consumption of these non-renewable fossil fuels generates carbon dioxide into the atmosphere causing the greenhouse effect. Therefore, the chemical industry must focus on the necessity to switch from the feedstock of fossil-fuel-based to the renewable resources. According to that, biomass, one of the suitable renewable carbon resources containing adequate carbon-carbon bonds to produce useful chemicals is a promising choice. The major component of the biomass, specifically, the lignocellulosic (wood, straw, and grasses) is the C₆-sugar (glucose, fructose, and mannose), which is an interesting precursor that can be used to produce a wide range of high value-added chemicals.

Regarding such chemicals, the lactic acid (2-hydroxypropionic acid, CH₃-CHOHCOOH) is an important natural organic acid that can be derived starting from biomass. It is widely used in the food, pharmaceutical, and cosmetic industries and also a building block for the synthesis of many useful chemicals such as pyruvic acid, acetaldehyde, acrylic acid, and propanoic acid [1].

Furthermore, it has received more attention in recent years because it is the feedstock for the manufacture of biodegradable plastics [poly(lactic acid), PLA], which can be decomposed by bacteria while exhibiting a good mechanical strength. Thus, it is a suitable choice for the replacement of petroleum-based polymers reducing the impact on the environment [2]. The worldwide demand for lactic acid is expected to increase rapidly in the near future. In 2008-2009, the largest PLA

producer has expanded its production capacity from 70,000 to 140,000 tons whereas the others are setting up pilot plants in China and Europe [3]. The market of lactic acid in the next seven years is expected to significantly grow which shown in Figure.1.1. The major factors that drive market growth are the rising demand for green packaging and environmental concern [4]. Moreover, PURAC (Corbion), the global leader company in lactic acid and lactic acid derivatives has just constructed the new 75,000-ton PLA plant in Thailand [5]. It is expected that lactic acid would be an important chemical in the future.

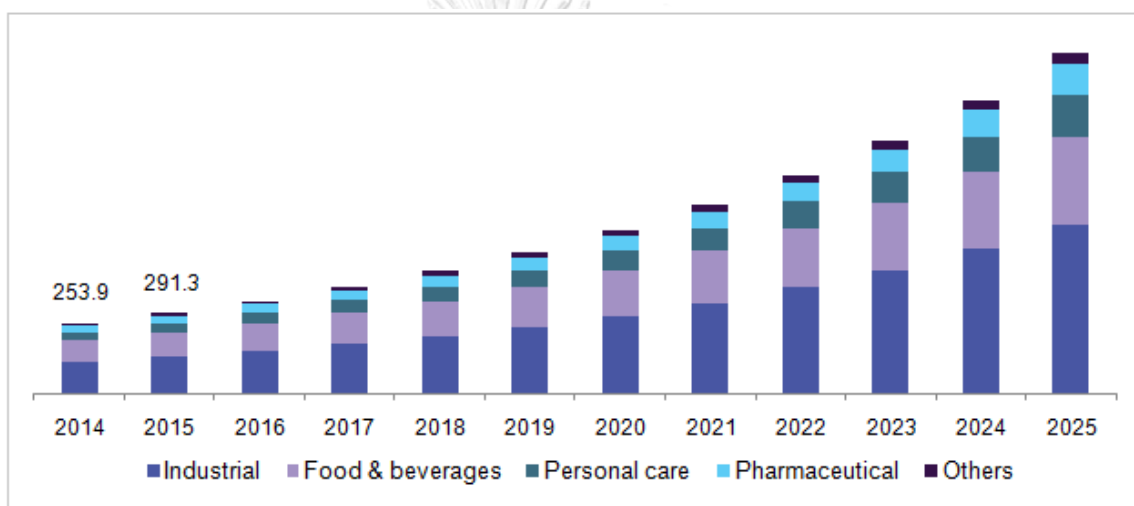


Figure 1.1 U.S. lactic acid market volume by application, 2014 - 2025 (Kilo Tons) [6]

The lactic acid can be synthesized by two routes: the fermentation of carbohydrates with microorganisms and the chemical synthesis. In the present, over 90% of the industrially-produced lactic acid is from the fermentation of glucose from starch utilizing an enzyme or microbes [7] because it shows advantages over the other route such as a low energy consumption. On the other hand, its drawbacks are that the process is time-consuming, needs strictly control environment, and needs multistep separation because it generates large amounts of wastes. Therefore, the chemical synthesis is an interesting choice. This process can generate the product in a shorter time, while the scale up to the industrial scale is less difficult.

Generally, in this route, the lactic acid was synthesized from petrochemical resources that include the hydrolysis of lactonitrile which was formed by the reaction between acetaldehyde and hydrogen cyanide. This process employed highly toxic cyanide causing environmental issues [8]. As a result, the lactic acid production from biomass resources and its derived carbohydrates by using the chemocatalytic systems rises as a more promising solution.

For the chemical processes, various studies chose the hydrothermal process which is performed in water at high temperature and pressure to utilize the water in the subcritical and supercritical region as an alkaline catalyst, while some reported the production of the lactic acid from sugars in an alkaline solution with or without metal catalyst [9]. But the alkaline reaction was always performed in extreme conditions which has some disadvantages including high energy consumption, increase equipment investment because it operates under high temperature and alkaline causes corrosion to reactor, limit the scaling-up and highly toxic to the environment. So, this research investigated heterogeneous catalytic conversion of glucose into lactic acid without alkaline solution, which the basicity in the reaction can obtain from heterogeneous catalyst.

From previous studies, many studies have reported the role of metal oxide which has divalent ions in the pathway of glucose conversion into lactic acid. In 2004, Huo *et al.* compared various transition metal ions including Ni^{2+} , Zn^{2+} , Co^{2+} , Fe^{2+} , Fe^{3+} , Mg^{2+} , Cd^{2+} , Sn^{2+} , and Cu^{2+} from metal chloride sources. The highest yields of 25% for lactic acid were obtained with the 0.01 M Ni^{2+} and 0.01 M NaOH at 300°C for 1 min [10]. In 2015, Choudhary *et al.* used magnesia supported-Cu oxide with hexadecyltrimethylammonium bromide (CTAB) as the capping agent as the catalyst. The optimum condition for the reaction was 120°C for 1 h with 2.5 M of NaOH, which provided 70% of lactic acid yield. They reported the role of Cu^{2+} in the pathway of lactic acid production from glucose, in which Cu^{2+} formed a complex with an intermediate and forced to produce the lactic acid [11]. Hence, this research used

various divalent transition metal oxide supported on magnesium oxide as a catalyst for the lactic acid production from glucose. The MgO was selected as support from the high basicity and a few leachates after performing in the reaction.

In term of the important role of basicity for the lactic acid production from glucose process, the effect of basicity from the solution and metal catalyst surface on this process was unclear. Thus, this research focuses on the study effects of basicity of solution and basicity of heterogeneous catalyst surface on glucose conversion and selectivity of lactic acid.

1.2 Objective

To investigate the effects of basicity of solution and basicity of heterogeneous catalyst surface on glucose conversion and selectivity of lactic acid.

1.3 The scopes of research

1.3.1 The various metal oxides having divalent ions (Cu, Co, Ni, and Zn) supported on MgO catalyst using CTAB as the capping agent with various metal loadings (1.5, 5, and 10 mmol/g-cat) were synthesized by the hydrothermal method.

1.3.2 The investigation of the effect of the catalyst on the lactic acid production from glucose including glucose conversion and selectivity of lactic acid was performed at various reaction temperatures (80, 100, 110, 120, and 140°C).

1.3.3 The products of the reaction were analyzed by High-Performance Liquid Chromatography (HPLC) with UV-detector.

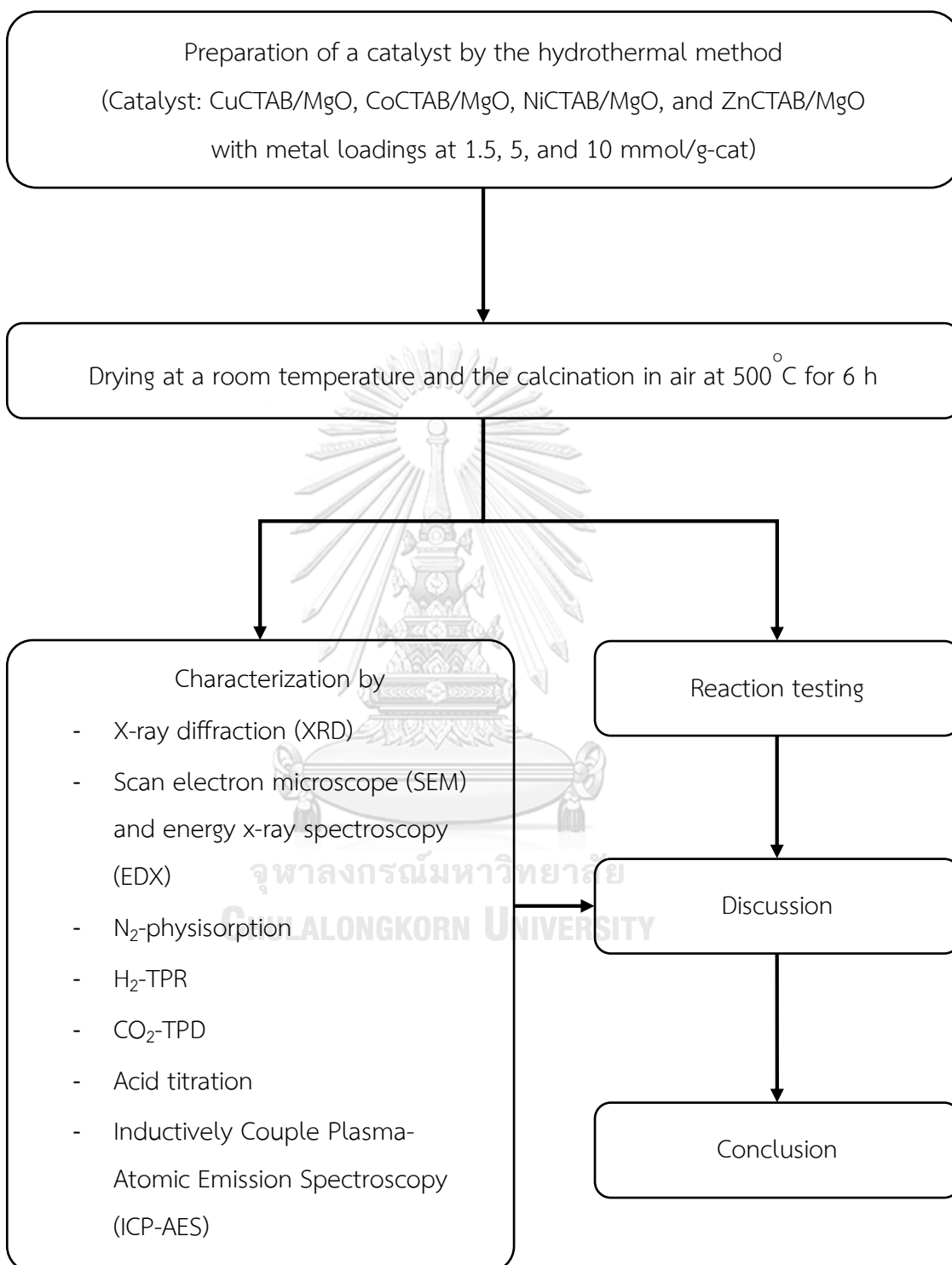
1.3.4 The catalysts were characterized by various techniques

1. X-ray diffraction (XRD)
2. Scan electron microscope (SEM) complied with energy x-ray spectroscopy (EDX)
3. N₂-physisorption

4. H₂ temperature programmed reduction (H₂-TPR)
5. CO₂ temperature programmed desorption (CO₂-TPD)
6. Acid titration
7. Inductively Coupled Plasma-Atomic Emission Spectroscopy (ICP-AES)



1.4 Research methodology



CHAPTER II

THEORY AND LITERATURE REVIEWS

This chapter described the information about the mechanism of the reaction, properties of the catalysts, and applications of the product in this work.

2.1 Lactic acid

2.1.1 Structure and properties of the lactic acid

The Lactic acid or 2-hydroxypropanoic acid is an organic chemical compound with a formula of $\text{CH}_3\text{CH}(\text{OH})\text{COOH}$. Its structure contains three carbon atoms with one terminal carbon atom of carboxyl group, while the other is the hydrocarbon group. It is classified as an alpha-hydroxy acid (AHA) because it has a hydroxyl group adjacent to the carboxyl group. It has two isomers: L-lactic acid or (s)-lactic acid and its mirror image, D-lactic acid or (r)-lactic acid shown in Figure 2.1, where a mixture of the two in equal amounts is called DL-lactic acid or racemic lactic acid [12, 13]. The L-Lactic acid is the biologically important isomer because it is a feedstock for manufacturer of biodegradable polylactic acid pastic. The Lactic acid is highly hygroscopic and usually handled in the concentrated solution (60–80% by weight) rather than in a solid form. The chemical and physical properties of lactic acid are summarized in Table 2.1.

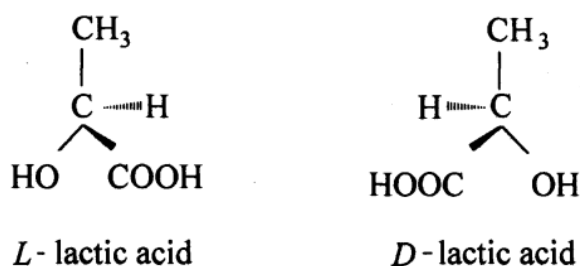


Figure 2.1 Lactic acid forms [12]

Table 2.1 The chemical and physical properties of lactic acid [14]

Properties	Values
Molecular Formula	CH ₃ CH(OH)COOH
Molecular Weight	90.078 g/mol
Density	1.2060 g/cm ³ at 21°C
Color	Viscous, colorless to yellow liquid or colorless to yellow crystals
Odor	Available forms have very slightly acid odor
Boiling Point	122°C at 15 mm Hg
Melting Point	16.8°C
Solubility	Completely soluble in water
	Completely soluble in ethanol, diethyl ether, and other organic solvents which are miscible with water
	Insoluble in benzene and chloroform
Vapor Pressure	0.0813 mm Hg at 25°C
Viscosity	36.9 cP (88.60 wt%) at 25°C

2.1.2 Applications of lactic acid

The Lactic acid has many applications, in which its various applications in the global market in the year 2014 was shown in Figure 2.2. The major parts of non-polymer grade lactic acid and its salt are used in the food industry. It is found primarily in sour milk products and sometime in candy, meat and sauces because it has a mild acidic taste. The Lactate salt is also used as an emulsifier in bakeries. Apart from the food industry, the lactic acid is widely used in the leather tanning, textile treatments, and pharmaceutical industry for the preparation of cosmetics such

as lotions, anti-acne solutions, and humectants. Also, It is also found in a small-scale industry including pH adjuster, terminating agent and lithographic printing [15].

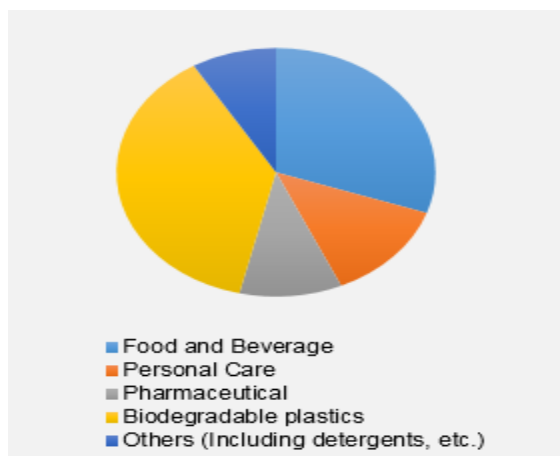


Figure 2.2 Global market of lactic acid in 2014 [16]

Moreover, the lactic acid is a strong oxidizer and highly reactive making it unsuitable for being a gasoline additive but an excellent building block for the synthesis of many useful chemicals shown in Figure 2.3.

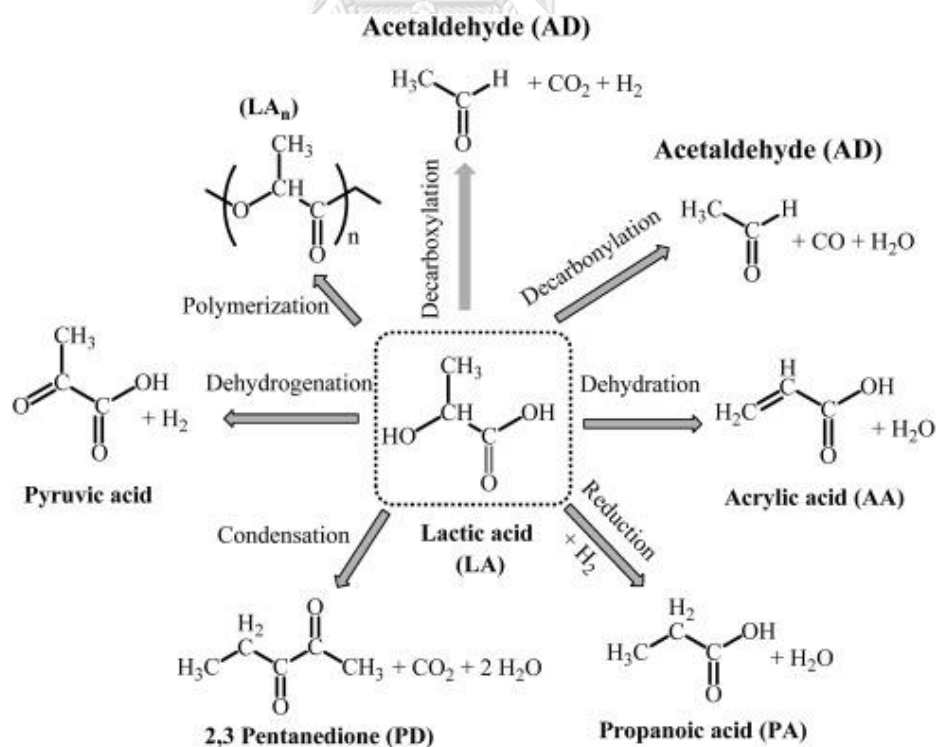


Figure 2.3 The role of lactic acid for the synthesis of useful chemicals [17]

The most prominent application of the lactic acid is its use as a raw material for the production of the polylactic acid (PLA) which is a thermoplastic biodegradable polyester. The PLA is usually synthesized from the cyclic lactide monomer by a ring-opening polymerization [18]. It is transparent, in which its degradation can be controlled by adjusting the composition and molecular weight of such plastic. Its characteristics are similar to that of the polypropylene (PP), polyethylene (PE), or polystyrene (PS) which are the petroleum-derived plastics. The applications range from the industrial packaging to fibers, clothes and biodegradable medical devices (such as screws and pins that are expected to biodegrade within 6-12 months) [19]. The example of PLA products was shown in Figure 2.4.



Figure 2.4 Poly-lactic acid products (a. Printing filament, b. Plastic cups and c. Medical screws) [19, 20]

2.1.3 The synthesis of lactic acid

Lactic acid can be produced either by microbial fermentation or chemical synthesis. In the present, over 90% of the commercial lactic acid production is

performed via the fermentation. Generally, a suitable carbohydrate source such as glucose, fructose which is derived from all kinds of starch is transformed into lactic acid by micro-organisms. This process offers advantages in terms of the production of optically selective L(+)-Lactic acid or D(-)-Lactic acid and its low energy consumption. Nonetheless, the reaction is time-consuming and it is difficult for the control of the bacteria population in the system together with the issue of the process scale-up [21].

Hence, another process of chemical synthesis is based on lactonitrile (2-hydroxypropanenitrile, CH_3CHOHCN) is of high interest. The Lactonitrile can be produced by adding the hydrogen cyanide into acetaldehyde in an alkaline media. The reaction is operated at high pressures in liquid phase. After the reaction, the crude of lactonitrile is obtained prior to the purification by the distillation before being hydrolyzed by the concentrated hydrochloric acid (HCl) or sulfuric acid (H_2SO_4) to produce the lactic acid product and the ammonium salt. In addition, this chemical synthesis process always produces a racemic mixture of DL-lactic acid [22, 23]. In conclusion, this process takes place under harsh condition making toxic causing environmental issue. Thus, the chemical synthesis using renewable resources instead of the lactonitrile has received more attention.

2.2 The chemocatalytic conversion of glucose into lactic acid

The process to produce lactic acid from glucose taking place in the reaction under the hydrothermal condition and mild condition with or without the alkali and heterogeneous catalyst were reported, where the details of the processes were described below.

2.2.1 Hydrothermal method

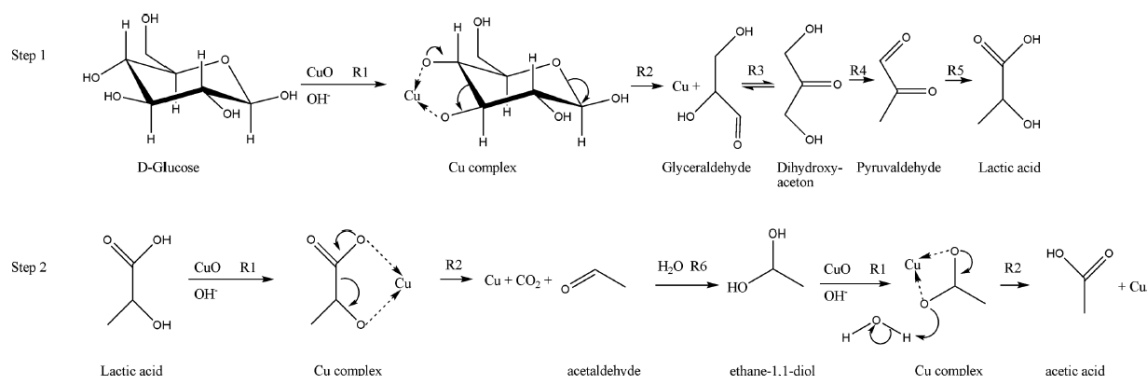
This method is the chemical reaction in water under high temperature and pressure [24].

2.2.1.1 Hydrothermal methods with an alkaline solution

Yan *et al.* (2007) studied the alkaline hydrothermal conversion of glucose into lactic acid by comparing two alkaline catalysts: NaOH and Ca(OH)₂. The reaction proceeded at 300°C for 60 s. The result showed that when the alkaline concentration was lowered, the production of lactic acid from the Ca(OH)₂ was more effective than that of the NaOH at the same OH⁻ concentration. However, at high alkali concentration, the Ca(OH)₂ did not lead to the increase in lactic acid yield. It is probably due to the low solubility of Ca(OH)₂. The highest lactic acid yield was obtained at 27% when 2.5 M NaOH is used and 20% when 0.32 M Ca(OH)₂ is used. From the economic viewpoint, the Ca(OH)₂ as an alkaline catalyst should be more suitable than NaOH [9].

2.2.1.2 Hydrothermal methods with heterogeneous catalyst and alkaline solution

Wang *et al.* (2013) studied the conversion of glucose into lactic acid and acetic acid with copper oxide (CuO) under hydrothermal conditions. They found that CuO greatly improves the yields of lactic acid and acetic acid from glucose. The CuO is an oxidant which was reduced to Cu₂O and Cu after the reaction. The possible mechanism was shown in Scheme 2.1, in which the strong base (NaOH) enhances the solubility of CuO forming the hydroxo complex under the hydrothermal condition. Afterwards, the Cu(II) ions in the hydroxo complex may coordinate with the hydroxyl oxygen atoms of glucose converting the glucose into lactic acid prior to the oxidation to acetic acid. In addition, Fructose, erythrose, glyceraldehyde, glycolaldehyde, and pyruvaldehyde were intermediates of the reaction. The highest yield of lactic acid and acetic acid (25% and 23%, respectively) were obtained at 300°C for 60 s with the addition of 1 M NaOH [25].



Scheme 2.1 Reaction pathway of production of lactic acid and acetic acid from D-glucose with CuO under alkaline hydrothermal conditions [25].

Adam *et al.* (2013) studied the effect of various metal oxides (CuO, Fe₃O₄, Fe₂O₃, Al₂O₃, ZnO, and TiO₂) on yields of carboxylic acids from glucose under the hydrothermal conditions. The result showed that the yields of lactic acid, formic acid and acetic acid in the presence of CuO or Fe₃O₄ were enhanced compared to other metal oxides, where the highest yield of lactic acid, acetic acid, and formic acid was 37.1%, 9.4%, and 4.9%, respectively. The reaction conditions were 300°C for 60 s with CuO 1.5 mmol and NaOH 2.5 M [26]. They suggested that CuO acts as an oxidant, while Fe₃O₄ acts as a catalyst in improving the conversion of glucose into carboxylic acids.

Huo *et al.* (2014) investigated the effect of transition metal ions on the selective conversion of glucose into lactic acid in a diluted aqueous NaOH solution. The various transition metal ions including Ni²⁺, Zn²⁺, Co²⁺, Fe²⁺, Fe³⁺, Mg²⁺, Cd²⁺, Sn²⁺, and Cu²⁺ which are obtained from their metal chloride. The highest yields of 25% for lactic acid were obtained with 0.01 M Ni²⁺ and 0.01 M NaOH at 300 °C for 1 min. From their XRD result, it was shown that after the reaction, the Ni²⁺ existed as Ni and Ni(OH)₂, which suggests that the Ni²⁺ acts not only as a catalyst but also as an oxidant in improving glucose conversion into lactic acid under hydrothermal conditions [10].

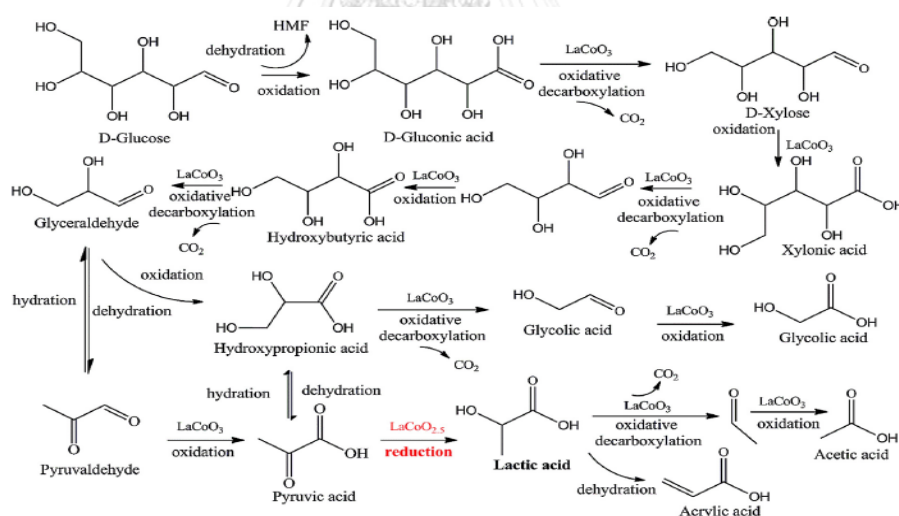
2.2.1.3 Hydrothermal methods with heterogeneous catalyst (without alkaline solution)

Xue *et al.* (2014) studied the effect of feldspars: Albite and Potassium feldspar as solid base catalysts on the lactic acid production from glucose. The highest lactic acid yield from this study is 12.37% and 10.84% when using Albite and Potassium feldspar, respectively. The reaction is carried out at 260°C, where the yields were observed at 100 s and 140 s. The catalytic activity of Albite before and after experiments is conserved but the crystal lattice of Potassium feldspar was destroyed in the first use [27].

Duo *et al.* (2016) studied the possibility and effectiveness of sodium silicate (Na_2SiO_3) as a base catalyst for glucose conversion into lactic acid because it's low cost, and it is an effective base catalyst in biodiesel production. They compared it with various catalysts including Na_2SiO_3 , MnO_2 , TiO_2 , NaHCO_3 , and $\text{Al}(\text{OH})_3$. From their result, the highest lactic acid yield (30%) was obtained when 0.6 mol/L Na_2SiO_3 , a reaction temperature of 300°C and reaction time of 60 s were used. They also reported that the decomposition of lactic acid to acetic acid and formic acid at the hydrothermal conditions may occur at a longer reaction time. The proposed reaction pathway was that the Na_2SiO_3 may be hydrolyzed producing the OH^- prior to the hydrothermal conversion of glucose into the lactic acid under an alkali condition. Moreover, they found that the use of Na_2SiO_3 led to a lower corrosion and higher lactic acid yield than that of the NaOH at the same pH [28].

Gao *et al.* (2016) using bentonite as a solid base catalyst in the hydrothermal conversion of glucose into lactic acid. Bentonite contains layered crystal structure of montmorillonite which has high cation exchange capacity. They expected that its Bronsted-base sites help convert the carbohydrate into the lactic acid. Their results showed that the bentonite acted as a base catalyst in promoting the lactic acid production, and improve the acetic acid production [29].

Yang *et al.* (2016) studied the effect of the redox properties of LaCoO_3 perovskite catalyst on the production of lactic acid from the cellulosic biomass. They found that the redox properties of the LaCoO_x catalyst play a central role in the conversion of sugars to lactic acid via a subcritical water, in which they proposed the reaction pathway shown in Scheme 2.2. First, the LaCoO_3 oxidized the aldehyde group in glucose to form gluconic acid, which is different from acid/base catalyzed glucose conversion reactions. Afterwards, the gluconic acid undergoes an oxidative decarboxylation and transforms into xylose. Additionally, the Xylose, xylonic acid, hydroxybutyric acid, and hydroxypropionic were generated in the same fashion. The Hydroxypropionic acid undergoes a dehydration reaction to produce pyruvic acid which further reduces to lactic acid. The perovskite structure is unchanged during the reaction. Thus, such regenerated perovskite catalyst can be reused. The highest yield of lactic acid was 40% at 200°C with an initial N_2 pressure of 2.76 MPa [30].

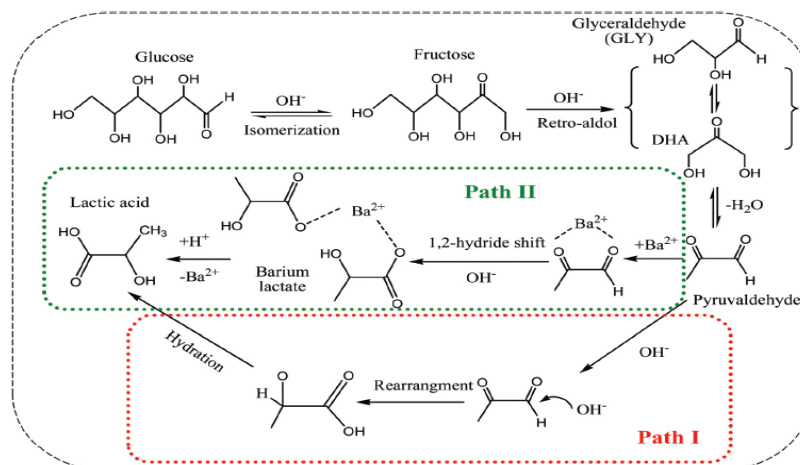


Scheme 2.2 A reaction pathway for LaCoO_3 catalytic conversion of glucose into lactic acid. [30]

2.2.2 The reaction under mild conditions

2.2.2.1 The reaction under mild conditions by using an alkaline solution

Li *et al.* (2017) selected common alkali metal hydroxides (NaOH and KOH) and alkaline-earth metal hydroxides (Mg(OH)_2 and Ba(OH)_2) to study the catalytic conversion of glucose in aqueous solutions. It was found that both NaOH and KOH were active for glucose conversion, while the Mg(OH)_2 was inactive, where this may be due to its low solubility in water. At the same OH^- concentration, the Ba(OH)_2 has greater catalytic activity than the NaOH and KOH. It is proposed that the divalent Ba^{2+} ion played an important role in the conversion of glucose into lactic acid. In addition, the reaction pathway was proposed in Scheme 2.3. In the beginning, the glucose was isomerized into fructose followed by the retro-aldol fragmentation forming the glyceraldehyde and dihydroxyacetone. Afterwards, the dehydration and re-arrangement of the glyceraldehyde to pyruvaldehyde takes place, in which it undergoes a methyl shift reaction producing the lactic acid. The role of Ba(OH)_2 may be attributed to its capacity to form a complex with pyruvaldehyde immediately after the dehydration of dihydroxyacetone. This complex transformed into lactic acid, wherein this occurs in a similar manner to the chemical transformations in the presence of the divalent ions. The highest lactic acid yield was 78.3% at 25°C for 48 h under a nitrogen atmosphere [31].



Scheme 2.3 Reaction pathway of the base-catalyzed the lactic acid production from glucose at room temperature under anaerobic conditions [31]

(Path I: general base catalyzed route; Path II: $\text{Ba}(\text{OH})_2$ catalytic – complex route)

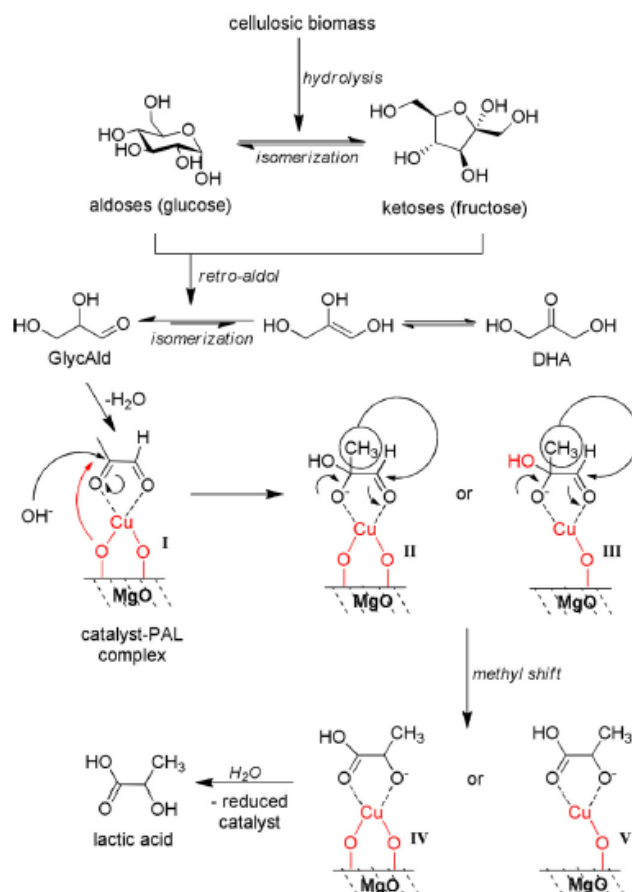
2.2.2.2 The reaction under mild conditions by using heterogeneous catalyst and alkaline solution

Onda *et al.* (2008) studied the selective conversion of D-glucose into lactic acid and gluconic acid by using the noble metal-supported catalysts with NaOH in an aqueous solution. The purpose of their study is to reduce the amounts of complex by-products which is formed in the alkaline degradations of D-glucose. They compared various metal-supported catalysts including Ru, Cu, Ag, Pd, and Pt supported on the activated carbon in the reaction at 80°C with the reaction time of 2 h under air bubbling. It was showed that the Pt/C gave the best activity to produce the lactic acid and gluconic acid, in which the obtained yield are 47 C% and 46 C%, respectively. The reason behinds a high activity found in the Pt/C might be due to its relatively high dispersion of platinum on support and high surface area. Also, the basicity of magnesium oxide and/or the interactions between the platinum and supports might contribute to this high catalytic activity. Moreover, it was also found that the NaOH concentration affected the alkaline degradation into lactic acid and the oxidation into gluconic acid [32]. In addition, their another study, which is the

Lactic acid production from glucose over activated hydrotalcites as solid base catalysts in water (2008) has shown that such catalyst of hydrotalcites which possesses the Brønsted-base sites shows high catalytic activity for aldol condensations.(the reaction in the pathway of glucose conversion into lactic acid in alkaline solution). Moreover, they investigated the effect of calcination temperature of the hydrotalcites catalyst in the production of lactic acid from glucose in a continuous process. It was reported that the highest lactic acid yield (20%) was obtained from the calcined hydrotalcite under air at 450°C, where the reaction was proceeded at 50°C for 8 h with 50 mmol/L of NaOH. They determined that the number of accessible Brønsted-base sites in the hydrotalcites depends on the calcination temperature and is linearly dependent of the activity of lactic acid production [33].

Choudhary *et al.* (2015) studied the conversion of sugars into lactic acid and formic acid promoted by Cu oxide on magnesia using CTAB as the capping agent. The catalyst was synthesized by a hydrothermal method for superior activity in the oxidation reaction. The result showed that the hydrothermal method makes the copper oxide species interacts strongly with the support, which prevents the formation of the free cationic copper. Also, they investigated the effect of calcination temperature on lactic acid production. From the result, the CuCTAB/MgO calcined at 500°C gave the highest yield for the lactic acid (53.4%) and exhibited the maximum number of Brønsted basic sites. Furthermore, they proposed the mechanistic pathways shown in Scheme 2.4. For this reaction, no pyruvaldehyde was observed. They suggested that the pyruvaldehyde was adsorbed onto the catalyst surface and formed catalyst–pyruvaldehyde complex (species I in Scheme 2.4). The attack of the OH⁻ ion of alkali or the binding oxygen atom of Cu–O–Mg from the catalyst on the carbonyl carbon may generate species II or III followed by the migration of the methyl group to the nearest carbon to produce species IV or V. They reported the crucial role of Brønsted basicity that, the need for a base in various steps in the

reaction pathway is important. The optimum conditions for CuCTAB/MgO (1mmolCu/g catalyst) were 120°C for 1 h with 2.5 M of NaOH, which provided 70% lactic acid yield [11].



Scheme 2.4 The mechanistic pathways for glucose conversion into a lactic acid by using Cu as a catalyst in the presence of alkali [11]

2.2.2.3 The reaction under mild conditions by using a heterogeneous catalyst (without alkaline solution)

Hou *et al.* (2015) developed $\text{Pb}(\text{OH})_2/\text{rGO}$ catalyst for the conversion of sugar to lactic acid using water as media. They found that the Pb^{2+} ion could catalyze the conversion of sugar into lactic acid efficiently. As a result, they were interested in fixing the $\text{Pb}(\text{OH})_2$ on the surface of a solid carrier (graphene) as an alternative catalyst. From various kinds of monosaccharide sugar and cellulose, the highest lactic

acid yield was reported from fructose (58.7%) at 190°C of 2 h reaction time under of 2.5 MPa of N₂ atmosphere, in which the catalyst can be effectively reused [34].

2.3 The important reaction in a base-catalyzed lactic acid production

2.3.1 Isomerization reaction

The Isomerization reaction is the transformation of one molecule into another molecule of the same number of atoms, but different arrangement, in other words, the transformation between its isomer [35]. As an example to the reaction, the isomerization of glucose to fructose by the alkali was shown in Figure 2.5. First, the alkali removes a proton (H⁺) from C2 (carbon labelled in blue) of the glucose molecule. The electron pair from the C-H bond migrate to form a C-C pi bond and another pair of electrons (from the C=O group) migrates to the carbonyl oxygen. Finally, fructose was obtained from the formation of the new C-O double bond on C2 and the migration of proton from the C2 hydroxyl group to C1 [36].

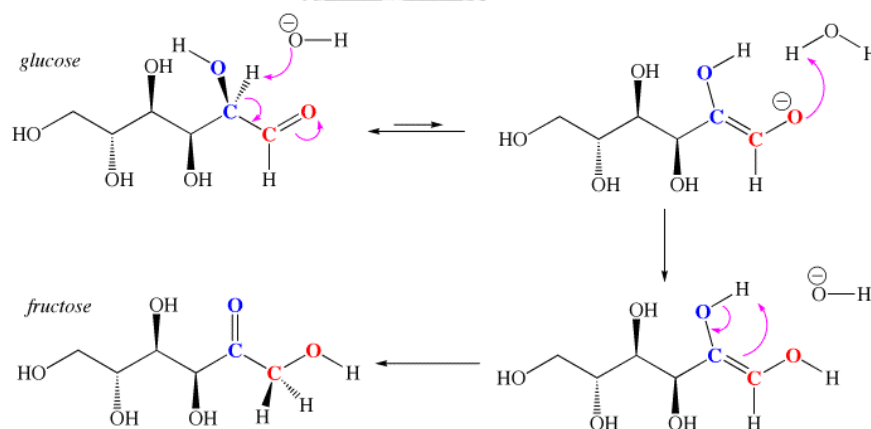


Figure 2.5 Isomerization of glucose to fructose in alkali [36]

2.3.2 The retro-aldol reaction

The retro-aldol reaction is the reverse process of the aldol reaction. Aldol reaction is a reversible organic reaction forming the C-C bonds via the combination of an enolate or enol and another carbonyl compound to form aldols, from the

combination of aldehyde and alcohol. The aldol reaction mechanism was shown in Figure 2.6 [37, 38].

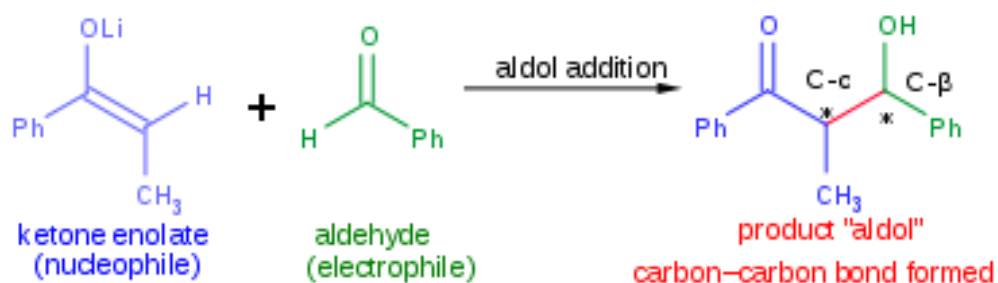


Figure 2.6 The aldol reaction mechanism [38]



CHAPTER III

EXPERIMENTAL

This chapter provided the details of the chemicals, catalyst preparation, reaction testing, and characterization.

3.1 Materials and chemicals

The details of the chemicals used in this research are shown in Table 3.1

Table 3.1 List of the chemical in this research

Chemicals	Formula	Brand
D(+)-Glucose	$C_6H_{12}O_6$	Vetec
D(-)-Fructose	$C_6H_{12}O_6$	Sigma-Aldrich
Lactic acid	$C_3H_6O_3$	Daejung
Magnesium oxide	MgO	Sigma-Aldrich
Copper(II) nitrate trihydrate	$Cu(NO_3)_2 \cdot 3H_2O$	Sigma-Aldrich
Cobalt(II) nitrate hexahydrate	$Co(NO_3)_2 \cdot 6H_2O$	Sigma-Aldrich
Nickel(II) nitrate hexahydrate	$Ni(NO_3)_2 \cdot 6H_2O$	Sigma-Aldrich
Zinc acetate dihydrate	$Zn(CH_3COO)_2 \cdot 2H_2O$	Sigma-Aldrich
Hexadecyltrimethylammonium bromide (CTAB)	$[(C_{16}H_{33})N(CH_3)_3]Br$	Sigma-Aldrich
Formic acid	HCOOH	Sigma-Aldrich
Acetic acid	CH_3COOH	Sigma-Aldrich

3.2 Catalyst preparation

The metal oxides supported on MgO catalysts using CTAB as the capping agent were synthesized by the hydrothermal method.

First, the MgO was dispersed in deionized water by sonication. Afterwards, an aqueous solution of various metals [$\text{Cu}(\text{NO}_3)_2 \cdot 3\text{H}_2\text{O}$, $\text{Co}(\text{NO}_3)_2 \cdot 6\text{H}_2\text{O}$, $\text{Ni}(\text{NO}_3)_2 \cdot 6\text{H}_2\text{O}$ or $\text{Zn}(\text{CH}_3\text{COO})_2 \cdot 2\text{H}_2\text{O}$] were added dropwise into the solution under vigorous stirring. Next, the addition of a CTAB solution into the mixture was done under vigorous stirring for 3 h (The ratio of metal to CTAB was 1:1). The mixture was added to a 3-L autoclave, heated to 180°C and maintained at this temperature for 24 h. After that, the cooling of the autoclave to room temperature was done slowly. The obtained solid was washed with deionized water until the pH of the filtrate solution is neutral, followed by the washing with ethanol. The drying of the solid was carried out at room temperature overnight before being calcined at 500°C for 6 h in air with the ramp rate of $10^\circ\text{C}/\text{min}$. The CTAB-capped-catalyst of various metal supported on MgO were obtained. All catalysts were controlled the particle size at $53 \mu\text{m}$, which was unaffected by internal mass transfer. Various catalysts were denoted as XYCTAB/MgO, where the X is the metal content in mmol per gram of catalyst (mmol/g-cat) and Y is the type of metal.

3.3 Catalytic reaction procedure

All of the catalytic reactions were conducted in a 50-mL Teflon-liner fitted stainless-steel autoclave. First, the loading of a 0.36 g catalyst into the autoclave was done. Then, a 0.54 g of glucose was dissolved into a 30-mL deionized water before adding the glucose aqueous solution into the catalyst. Next, the autoclave was sealed, followed by the purging with nitrogen three times at 0.4 MPa. After the introduction of N_2 , the autoclave was placed in a preheated oil bath. The mixture was stirred with a magnetic stirrer at 400 rpm (unaffected by external mass transfer) and reacted at various temperatures for 1 h. After the reaction, the autoclave was

allowed to cool down to a room temperature in an ice-water bath immediately. The resulting solution was filtrated with a 0.2 μm syringe filter and was analyzed by a high-performance liquid chromatography (HPLC).

3.4 Product analysis

The resulting solution was analyzed by a high performance liquid chromatography (HPLC), Agilent LC 1100 equipped with UV-detector using Agilent Hiplax-H column. For a UV-detector, a wavelength of 195 nm was used to detect sugars (glucose, fructose) and a wavelength of 210 nm was used for detecting the organic acids (lactic acid, formic acid, and acetic acid) [39]. The dilute sulfuric aqueous solution of 5 mM in deionized water was used as the mobile phase at a flow rate of 0.6 mL/min. The conversion and yield were determined using the calibration curve.

The glucose conversion and yield of organic acid were calculated from the following equations;

$$\text{Conversion (\%)} = \frac{\text{Mole}_{\text{glucose, in}} - \text{Mole}_{\text{glucose, out}}}{\text{Mole}_{\text{glucose, in}}} \times 100$$

$$\text{Selectivity}_i (\%) = \frac{\text{Mole}_{i, \text{out}} \times \text{Number of carbon in product}}{(\text{Mole}_{i, \text{in}} - \text{Mole}_{i, \text{out}}) \times \text{Number of carbon in substrate}} \times 100$$

3.5 Catalyst characterization

Several characterization techniques were used in this research to understand the structure and properties of the catalyst. The details for each technique were described below.

3.5.1 X-ray diffraction (XRD)

The crystal structure and X-ray diffraction (XRD) patterns were analyzed by an X-ray diffractometer (Bruker D8 Advance) using the Cu $K\alpha$ irradiation at a range

between 10 ° and 80 ° with a step of 0.05 °/s. The lattice parameter and d-spacing were calculated based on Bragg's law. Crystallite size was calculated by the Scherrer equation.

3.5.2 Scan electron microscope (SEM) and energy x-ray spectroscopy (EDX)

The SEM-EDX was used to determine the elemental distribution on a surface of the catalysts using Link Isis series 300 program SEM (JEOL model JSM-5800LV).

3.5.3 N₂-physisorption

The specific surface area was determined through a nitrogen adsorption-desorption method using a Brunauer-Emmett-Teller (BET) model in a Micromeritics Chemisorb 2750. The catalyst was pretreated under pure N₂ at 200°C for 1 h. Then, the 30% of N₂/He mixture (carrier gas) flowed through the sample, followed by the cooling of the catalyst under liquid nitrogen. During this step, 30% of N₂/He mixture was adsorbed on the catalyst surface until completion. Finally, the catalyst was left to desorb nitrogen at room temperature. The amount of nitrogen desorption was measured to investigate the specific surface area.

3.5.4 H₂ temperature programmed reduction (H₂-TPR)

The H₂-TPR was used to determine the reducibility of the catalyst. In such experiment, a 0.08 g of catalyst was placed into the U-tube quartz reactor and pretreated under nitrogen (flow of 25 ml/min) at 250°C for 1 h to remove the water and impurity in the catalyst. After the cooling down to 30°C, the catalyst was heated from a room temperature to 650 °C at a rate of 10 °C/min under a flow of 10%H₂/Ar mixture (flow of 25 ml/min). The consumption of H₂ was recorded by the TCD.

3.5.5 CO₂ temperature programmed desorption (CO₂-TPD)

The CO₂-TPD was used for the measurement of the catalyst basicity. Each catalyst (0.1g) was charged into the U-tube quartz reactor. It was pretreated to 450°C

with a temperature increase of 10°C/min and held for 1 h under a flow of Helium at 25 mL/min to remove any physisorbed organic molecules. Then, it is cooled down to 60°C followed by the saturation by CO₂ (flow at 25 mL/min) for 30 min. Afterwards, the gas was changed to helium (25 mL/min) to remove the physisorbed CO₂. When the baseline was constant, the temperature of the furnace was increased to 750°C with a temperature increase of 10°C/min under a helium flow of 25 mL/min. The obtained TPD profile was recorded with a thermal conductivity detector (TCD) (Micromeritics 2750).

3.5.6 Acid titration

To investigate the basicity of catalyst in liquid phase, the titration with benzoic acid was selected. The catalyst 0.025 g of each catalyst was dispersed in 5 mL mixed solution of ethanol and water in the ratio of 1:4 V/V in the Erlenmeyer flask, followed by the addition of the phenolphthalein 1-2 drops to the solution as an indicator. Then, 0.5 M benzoic acid was added dropwise until the color of solution was changed from pink to colorless. The amount of basic site was calculated from the volume of used benzoic acid (mmol/g-cat).

3.5.7 Inductively Coupled Plasma-Atomic Emission Spectroscopy (ICP-AES)

The optima 2100 DV spectrometer was employed to quantify the actual amount of metal deposited on the MgO and evaluate the leaching of the metal from the catalyst during the reaction. The catalyst was digested into a solution phase before the estimation of the metal contents using a calibration curve method.

CHAPTER IV

RESULTS AND DISCUSSION

This chapter shows the results and discussion of this research that consisted of three parts. The first part explained the effects of type of divalent metal oxide supported on MgO using CTAB as the capping agent on the glucose conversion and selectivity of lactic acid, in which the divalent metal oxides are Cu, Co, Ni, and Zn loading at 1.5 mmol/g-cat. The second part investigated the effects of amounts of metal loading on MgO at 1.5, 5, and 10 mmol/g-cat on the glucose conversion and selectivity of lactic acid. The last part explained the proposed mechanism of each catalyst for the lactic acid production process. The catalysts were prepared via the hydrothermal method, where they were characterized by the XRD, SEM-EDX, N₂-physisorption, H₂-TPR, CO₂-TPD, titration with benzoic acid, and ICP techniques.

4.1 Effects of the type of divalent metal oxide supported on MgO catalysts on the lactic acid production from glucose

The various metal oxide supported on MgO catalysts with metal loading at 1.5 mmol/g-cat are discussed in this part.

4.1.1 The physical and chemical properties of catalysts

4.1.1.1 X-Ray Diffraction (XRD)

The XRD patterns of fresh and first used various metal oxide supported on MgO catalysts for lactic acid synthesis at 140°C, 1 h within the 2θ range of 20°-80° are shown in Figure 4.1 and 4.2, respectively.

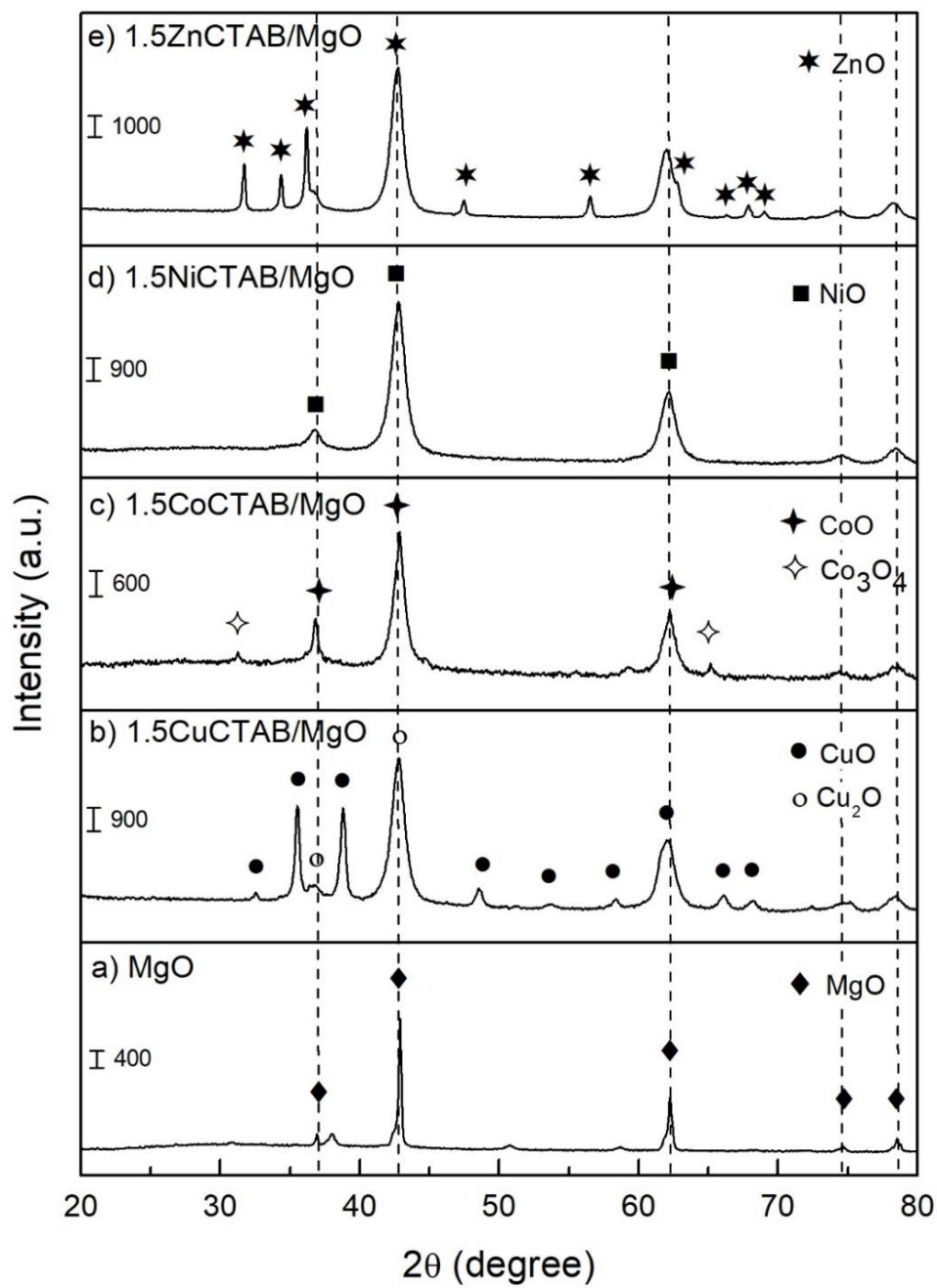


Figure 4.1 XRD patterns of fresh metal oxide supported on MgO catalysts with metal loading at 1.5 mmol/g-cat

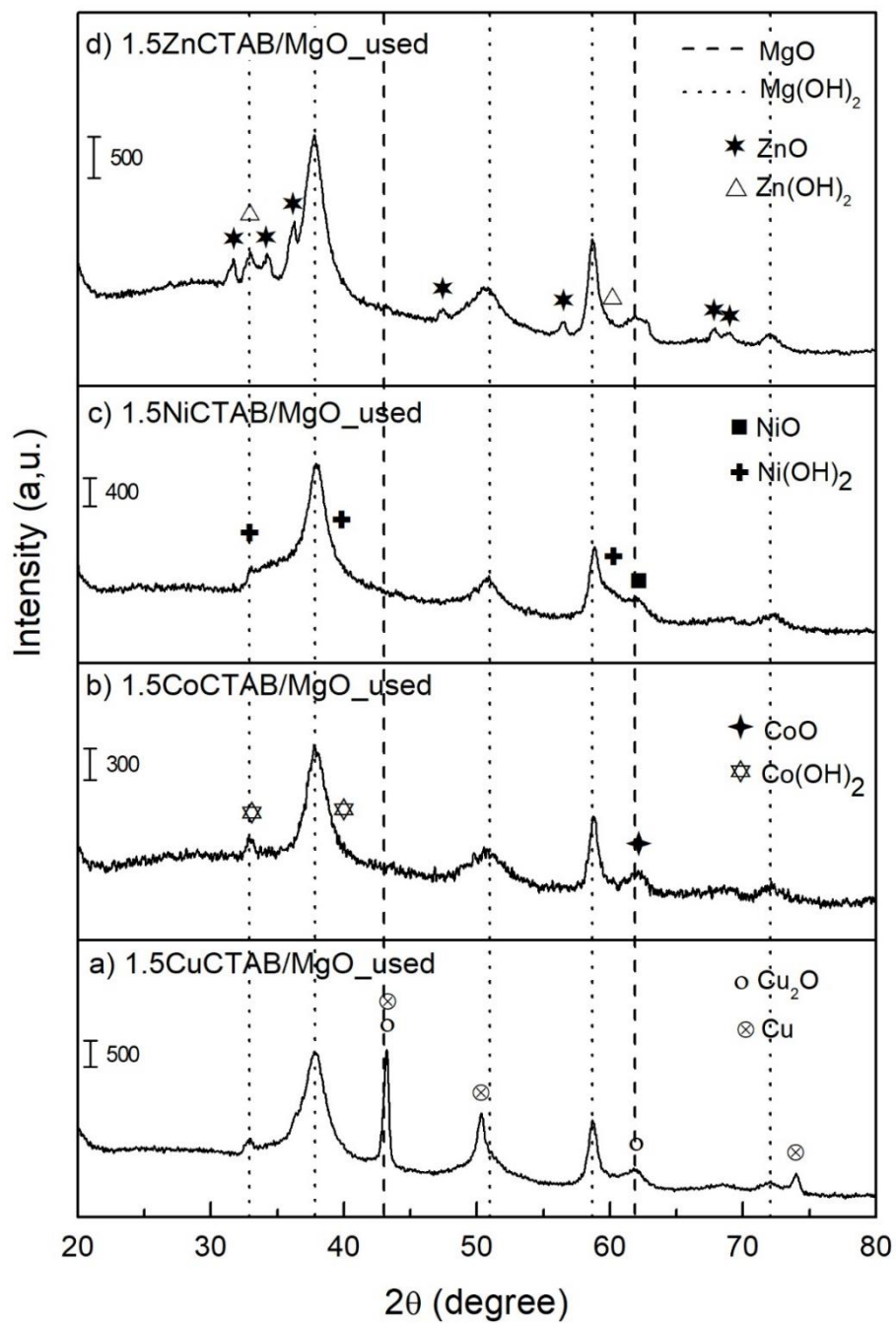


Figure 4.2 XRD patterns of used metal oxide supported on MgO catalysts with metal loading at 1.5 mmol/g-cat in the lactic acid synthesis from glucose at 140°C for 1 h

From Figure 4.1, all of the fresh catalysts displayed the characteristic peaks at 2θ angle of 36.9° (111), 42.9° (200), 62.3° (220), 74.7° (311), and 78.6° (222) assigned to the cubic structure of the MgO [40]. After each metal was loaded to the MgO, the characteristic peaks of various metal oxide were observed. For CuCTAB/MgO catalyst (Figure 4.1b), both of Cu₂O and CuO characteristic peaks were shown. The peaks at 36.4° and 39.5° corresponded to the (002) and (200) planes revealed the presence of CuO crystallites in the catalyst [11]. For CoCTAB/MgO catalyst (Figure 4.1c), there were three main peaks at 36.6° , 42.5° , and 61.6° which associated with the (111), (200) and (220) planes of the spinel phase CoO. The minor peaks at 31.3° (220) and 65.2° (440) suggested being the Co₃O₄ [41, 42]. NiCTAB/MgO (Figure 4.1d) showed all characteristic peaks of NiO which were aligned with the peaks of the MgO at 36.8° , 42.8° , and 62.2° . And the characteristic peaks of ZnCTAB/MgO (Figure 4.1e) showed the ZnO peaks at 31.7° , 34.4° , 36.2° , 47.4° , 56.5° , 62.0° , 67.8° , and 69° corresponded to the (100), (002), (101), (102), (110), (103), (200), and (112) planes confirmed the hexagonal structure of ZnO [43]. From XRD patterns of fresh catalyst, it is noticeable that the peaks of all metal oxide species were a coincidence with the peaks of MgO indicated that the CuO, CoO, NiO, and ZnO were supported successfully on the MgO with no impurity presented.

For the catalyst after first used in lactic acid synthesis from glucose at 140°C , 4 bar for 1 h (Figure 4.2), the XRD pattern of all catalysts are shown the characteristic peaks at 2θ angle of 32.9° , 38.1° , 50.9° , 58.7° , and 72.1° which corresponded to Mg(OH)₂ phase [44]. It suggests that the MgO phase in fresh catalyst transform to Mg(OH)₂ phase after used in the reaction. The MgO is an active species that can react with water at a low temperature to produced Mg(OH)₂ [45]. For CuCTAB/MgO catalyst after used in the reaction (Figure 4.2a), the peaks located at 43.21° (111), 50.37° (200), and 74.0° (220) are assigned to the metallic Cu. This is related to the report of Choudhary et al. (2015), the metallic Cu occurred from the reduction of CuO during the reaction to produce lactic acid, as the proposed mechanistic pathway in Scheme

2.4 [11]. The CoCTAB/MgO showed peaks of Co(OH)_2 at 33.0° (100) and 38.5° (101) and remained peak of CoO suggested that the Co_3O_4 was reduced to CoO during the reaction. While NiCTAB/MgO and ZnCTAB/MgO are not found any peak of metallic species, there were characteristic peaks of metal oxide and metal hydroxide. The NiCTAB/MgO showed peaks of Ni(OH)_2 at 33.2° (100), 38.6° (011), and 59.3° (110) while ZnCTAB/MgO exhibited peaks at 32.8° and 59.5° corresponded to Zn(OH)_2 [46-48]. This suggested that when NiCTAB/MgO and ZnCTAB/MgO was added into water, the NiO and ZnO were chemisorbed by water molecule generated Ni(OH)_2 and Zn(OH)_2 at the surface of the catalyst. At the catalyst surface, Ni^{2+} and Zn^{2+} act as water adsorption sites. The dissociation of a water molecule into the $\cdot\text{H}$ and $\cdot\text{OH}$ radicals chemisorbed to ions on the ZnO and NiO surface. The hydroxyl group ($\cdot\text{OH}$) bonds to metal atom on the NiO and ZnO surface generates the Ni(OH)_2 and Zn(OH)_2 species on the surface of catalyst [49, 50]. The proposed mechanistic pathway for each catalyst will be described in section 4.3.

4.1.1.2 Scan electron microscope (SEM) and energy x-ray spectroscopy (EDX)

The morphology and element compositions over the catalyst surface of various metal oxide supported on MgO catalysts with metal loading at 1.5 mmol/g-cat were determined by SEM and EDX (Table 4.1 and Figure 4.3).

Table 4.1 The elemental compositions of various metal loading on MgO catalysts from energy X-ray spectroscopy

Catalysts	Weight% (mmol/g-cat)					
	Mg	O	Cu	Co	Ni	Zn
CuCTAB/MgO	51.72	40.52	7.76 (1.22)	-	-	-
CoCTAB/MgO	53.89	38.89	-	7.22 (1.20)	-	-
NiCTAB/MgO	53.60	40.40	-	-	6.00 (1.02)	-
ZnCTAB/MgO	52.53	39.65	-	-	-	7.82 (1.20)

The element compositions from EDX measurement showed that all catalysts have metal loading at the surface lower than the desired content. The NiCTAB/MgO exhibited the lowest loading of 1.02 mmol/g-cat, while the others have similar content (around 1.2 mmol/g-cat). This may be due to the ability of metals to be supported on MgO which affected by the crystal growth behavior of each metal. The different metals have different behavior; Therefore, it is difficult to synthesize the catalysts with the similar metal content at the same calcination temperature [40]. From Figure 4.3, the SEM images revealed that the morphology of all catalysts have an irregular shape with the different sizes and EDX map indicated the good dispersion of metal on the surface for all catalysts.

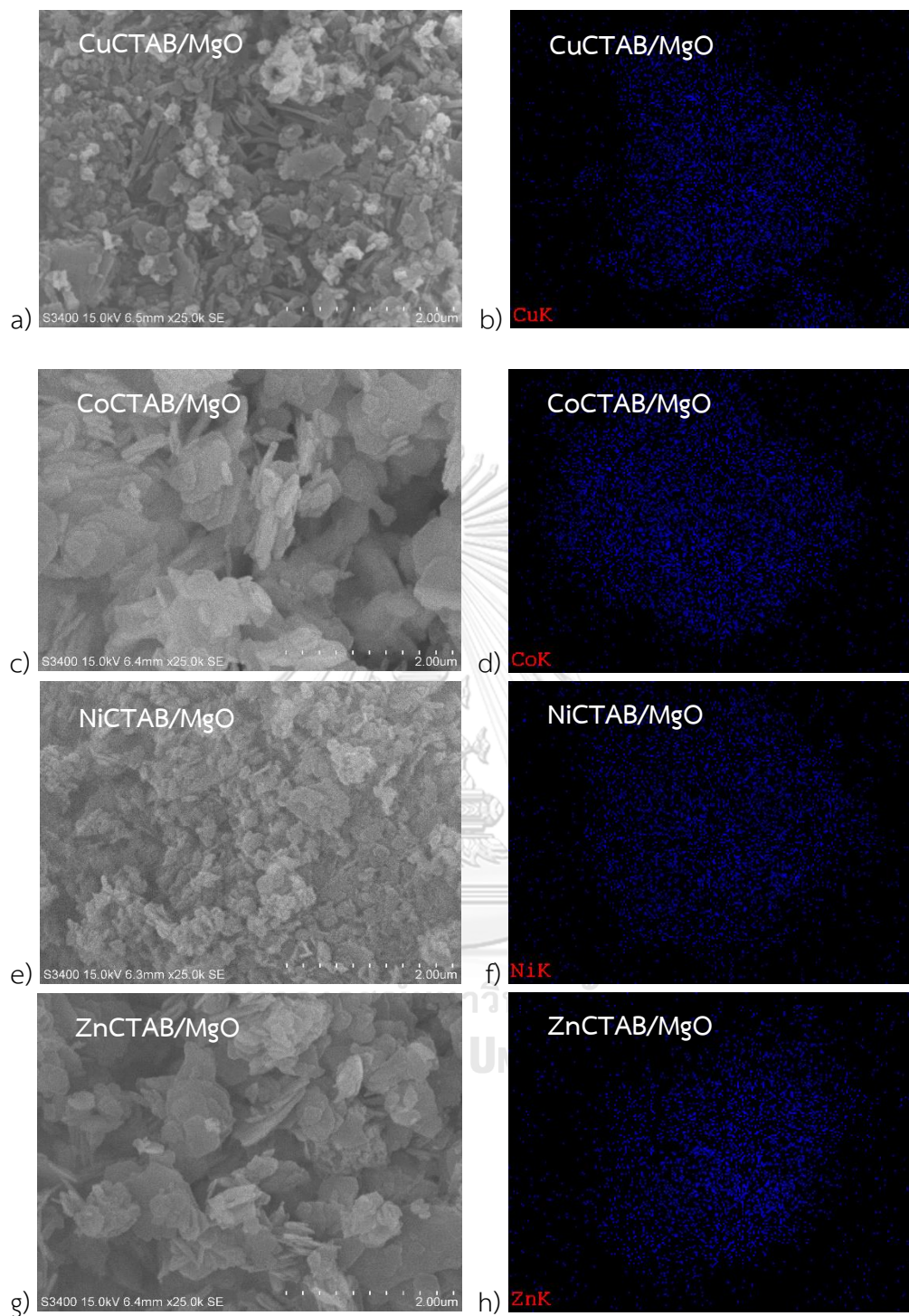


Figure 4.3 SEM images and EDX maps of metal oxide supported on MgO catalysts with metal loading of 1.5 mmol/g-cat

4.1.1.3 N₂-physisorption

The specific surface area of the catalysts with metal loading at 1.5 mmol/g-cat were measured by a Micromeritics Chemisorb 2750 are shown in Table 4.2.

Table 4.2 The specific surface area of the catalysts with metal loading at 1.5 mmol/g-cat

Catalyst	Surface area (m ² /g)
MgO	187.2
CuCTAB/MgO	162.2
CoCTAB/MgO	134.5
NiCTAB/MgO	132.1
ZnCTAB/MgO	94.5

From table 4.2, MgO showed the highest specific surface area of 187.2 m²/g, while the surface area of catalysts with metal loading were decreased. These results suggest that the oxide of metal blocked the pores of the catalyst support, which lead to the decrease in specific surface area.

4.1.1.4 H₂ temperature programmed reduction (H₂-TPR)

To understand the reducibility of catalyst, the H₂-TPR was employed. The H₂-TPR profiles of various metal oxide supported on MgO catalysts are shown in Figure 4.4.

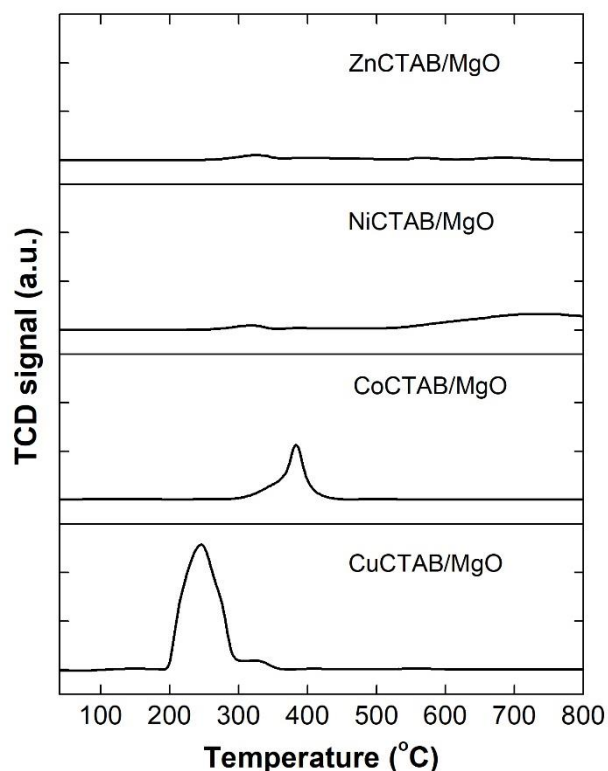


Figure 4.4 H₂-TPR profiles of metal oxide supported on MgO catalysts

As a result, the H₂-TPR profiles of NiCTAB/MgO and ZnCTAB/MgO exhibited smaller peaks than those of CuCTAB/MgO and CoCTAB/MgO. This suggested that NiCTAB/MgO and ZnCTAB/MgO were hardly reduced by hydrogen compared with the others. These profiles were consistent with the XRD patterns of used NiCTAB/MgO and ZnCTAB/MgO catalyst, in which the characteristic peaks of metallic Ni and Zn were not observed. While, CoCTAB/MgO showed a reduction peak at 360-400°C, which is ascribed to the reduction of Co₃O₄ [51]. The CuCTAB/MgO exhibited a peak at low temperature. It indicated that CuCTAB/MgO can be reduced easier than the others according to the presence of metallic Cu species in the XRD pattern of used CuCTAB/MgO catalyst. The H₂ consumption profile of CuCTAB/MgO showed peaks at 220°C, 270°C, and 320°C, indicating the different redox behaviors of the CuO species. The peaks at 220°C attributed to a well-dispersed CuO phase which can be easily

reduced and the peak of 260°C has reflected the reduction of larger CuO particles. Another broad peak at 300-330°C was due to a low metal dispersion [52, 53].

4.1.1.5 CO₂ temperature programmed desorption (CO₂-TPD)

The basicity properties of surface catalysts were investigated by CO₂-TPD technique. The CO₂-TPD profiles of pure MgO and various metal oxide supported on MgO catalysts are shown in Figure 4.5 and the amounts of total basicity which calculated from the amounts of total CO₂ desorption are shown in Table 4.2.

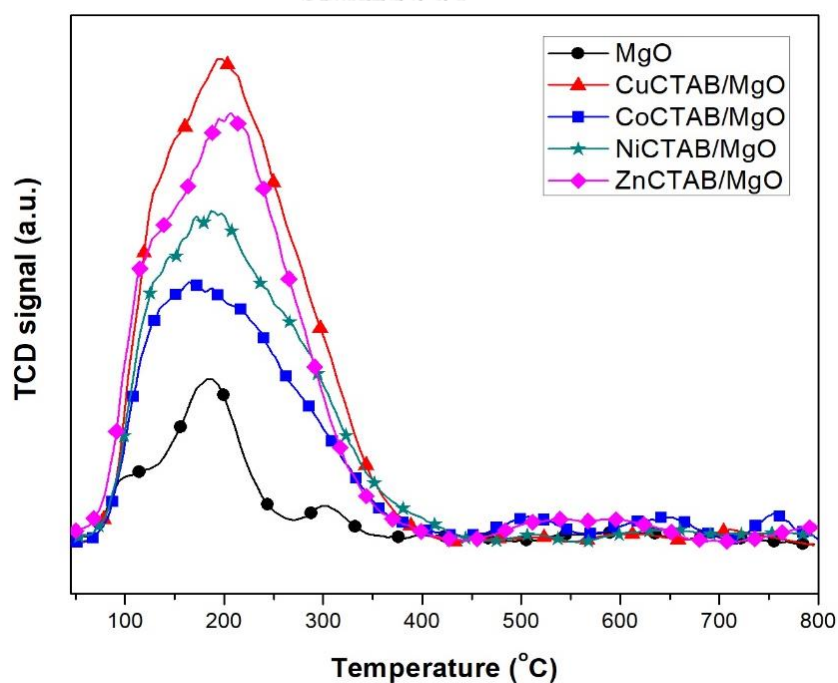


Figure 4.5 CO₂-TPD profiles of MgO and metal oxide supported on MgO catalysts

Table 4.3 Amounts of total basicity of MgO and metal oxide supported on MgO catalysts which calculated from CO₂-TPD technique

Catalyst	Amounts of total basicity ($\mu\text{mol CO}_2/\text{g.cat.}$)
MgO	116.8
CuCTAB/MgO	462.6
CoCTAB/MgO	259.7
NiCTAB/MgO	343.3
ZnCTAB/MgO	403.2

As shown in Figure 4.4, all catalysts were clearly observed the CO₂ desorption peaks at the temperature lower than 300°C and pure MgO showed another small peak at 300°C. This indicated that metal oxide supported on MgO catalysts have a weak basic site on the surface of the catalysts. The trend in the amounts of basicity, which calculated from the intensity of CO₂ desorption peak was in the order of CuCTAB/MgO > ZnCTAB/MgO > NiCTAB/MgO > CoCTAB/MgO > MgO.

4.1.1.6 Acid titration จุฬาลงกรณ์มหาวิทยาลัย

To investigate the basicity of the surface catalyst in water, the titration with benzoic acid was employed. The amounts of total basicity from various metal oxide supported on MgO catalysts are shown in Table 4.3.

Table 4.4 Amounts of basicity of fresh and used MgO and metal oxide supported on MgO catalysts which calculated from acid titration technique

Catalyst	Acid titration (mmol/g-cat)	
	Fresh	Used
CuCTAB/MgO	3.8	1.3
CoCTAB/MgO	1.9	0.9
NiCTAB/MgO	2.6	1.7
ZnCTAB/MgO	4.8	2.0
MgO	1.45	0.5

From Table 4.3, the trend of basicity from the titration with 0.05 M benzoic acid was shown as ZnCTAB/MgO > CuCTAB/MgO > NiCTAB/MgO > CoCTAB/MgO. It's noticeable that CuCTAB/MgO exhibited the highest basicity from CO₂-TPD technique, while ZnCTAB/MgO showed the highest basicity from acid titration technique. This suggested that the basicity of ZnCTAB/MgO increased from the chemisorption of the hydroxyl group at the surface of the catalyst when the catalyst was added into water.

4.1.1.7 Inductively Coupled Plasma-Atomic Emission Spectroscopy (ICP-AES)

The leachates of metal from catalysts after used in the lactic acid production from glucose were analyzed by ICP-AES technique. The amounts of metal leaching from MgO and metal oxide supported on MgO catalysts at various reaction temperature are shown in Table 4.4. The amounts of metal leaching from lactic acid production from glucose at all reaction temperature have a similar trend as MgO > NiCTAB/MgO > ZnCTAB/MgO > CuCTAB/MgO > CoCTAB/MgO.

Table 4.5 Amounts of metal leaching from lactic acid production from glucose

Catalyst	Temperature (°C)	Amount of leaching (μmol)		
		Metal	Mg	SUM
CuCTAB/MgO	80	0.2	46.6	46.8
CoCTAB/MgO	80	0.2	37.4	37.6
NiCTAB/MgO	80	0.2	56.8	57.0
ZnCTAB/MgO	80	0.3	47.2	47.4
MgO	80	0.0	59.1	59.1
CuCTAB/MgO	100	0.3	131.9	132.2
CoCTAB/MgO	100	0.2	116.3	116.5
NiCTAB/MgO	100	0.6	147.1	147.7
ZnCTAB/MgO	100	0.7	142.1	142.8
MgO	100	0.0	191.0	191.0
CuCTAB/MgO	110	0.1	261.9	262.0
CoCTAB/MgO	110	8.4	205.9	214.2
NiCTAB/MgO	110	19.3	255.3	274.6
ZnCTAB/MgO	110	15.1	250.1	265.2
MgO	110	0.0	299.3	299.3
CuCTAB/MgO	120	0.4	291.6	292.1
CoCTAB/MgO	120	13.2	272.8	286.0
NiCTAB/MgO	120	56.5	238.6	295.1
ZnCTAB/MgO	120	51.6	242.6	294.2
MgO	120	0.0	307.0	307.0
CuCTAB/MgO	140	0.3	343.2	343.5
CoCTAB/MgO	140	17.6	315.0	332.6
NiCTAB/MgO	140	31.5	334.6	366.1
ZnCTAB/MgO	140	46.4	302.2	348.6
MgO	140	0.0	410.1	410.1

4.1.2 Catalytic performance for lactic acid production from glucose

The effects of type of metal oxide supported on MgO catalysts and alkaline solution (Sodium hydroxide, NaOH) on glucose conversion and selectivity of lactic acid as a function of reaction temperature are shown in Figure 4.6 and 4.7, respectively.

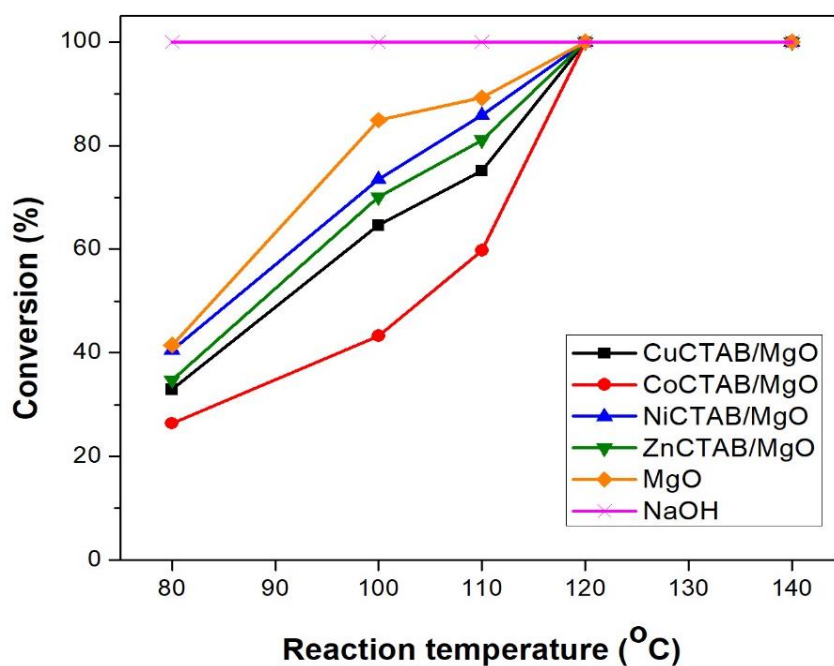


Figure 4.6 Catalytic activity of metal oxide supported on MgO catalysts at the various reaction temperature

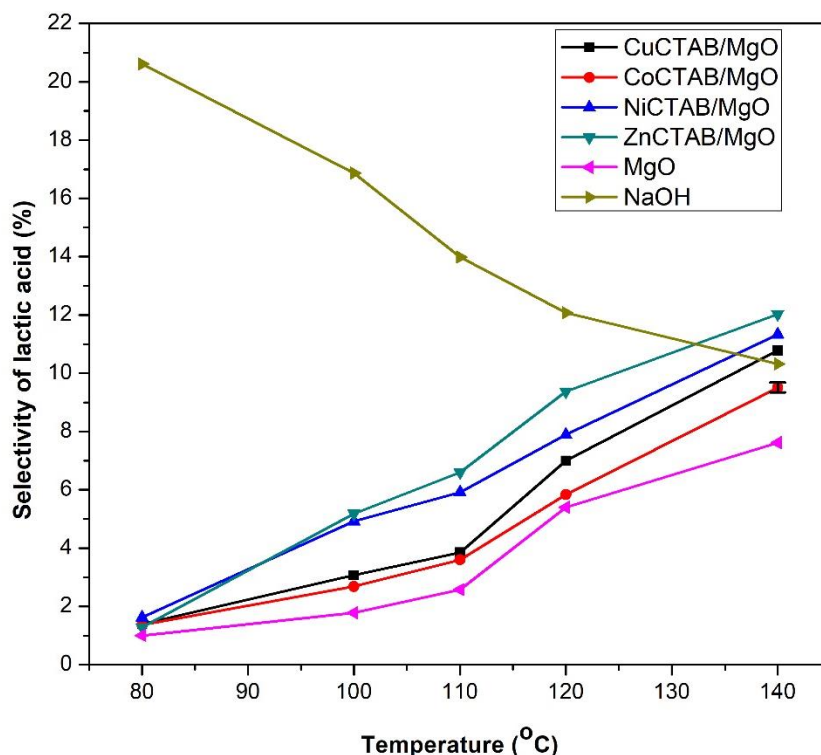


Figure 4.7 Selectivity of lactic acid of metal oxide supported on MgO catalysts at the various reaction temperature

From Figure 4.6, the heterogeneous catalysts including MgO, CuCTAB/MgO, CoCTAB/MgO, NiCTAB/MgO, and ZnCTAB/MgO have a similar trend. Glucose conversion of all catalysts increased with an increase in the reaction temperature and reached 100% at 120°C. This suggested that the increase in the reaction temperature gave higher energy in the dissection of glucose molecules into smaller molecules and the increasing of metal leachate from the catalyst. The pure support (MgO) has higher activity in the conversion of glucose than the support doped with metal oxide catalysts. The high activity of MgO may come from a large amount of Mg leachate in the solution after used in the reaction compared with the metal oxide supported on MgO catalysts. The Mg ion from the leaching of catalyst affected the conversion of glucose [54]. From the ICP results, it can be suggested that the capping agent (CTAB) which added to metal oxide supported on MgO catalysts can be prevented the metal leaching from the catalyst and also improved the stabilized of

metal onto MgO support [11]. Among of metal oxide supported on MgO catalysts, the catalytic activity is showed follow the trend as NiCTAB/MgO > ZnCTAB/MgO > CuCTAB/MgO > CoCTAB/MgO which related with the leachate from ICP results. Moreover, the basicity from acid titration of leachate solution of MgO was 0.6 mmol/g-cat, which was higher than the basicity of metal oxide supported on MgO catalysts (0.2-0.4 mmol/g-cat). Wang *et al.* (2013) reported the isomerization reaction from glucose can be catalyzed by metal ion or metal hydroxide [55]. It's indicated that the metal ion and the basicity in the solution affected glucose conversion more than the basicity at the catalyst surface. In term of the homogeneous catalyst which represented by solution of NaOH, Glucose conversion was 100% at all reaction temperature. When NaOH was dissolving in water, it dissociated to OH⁻ and Na⁺ molecules. The hydroxyl ion catalyzed the glucose isomerization process making a high activity for glucose conversion [56].

The selectivity of lactic acid from the metal oxide catalysts and the solution of NaOH as a function of the reaction temperature are shown in Figure 4.7. The selectivity of lactic acid obviously low at all temperature. In the case of heterogeneous catalysts without alkaline solution additive, the main product was fructose at a temperature below 120°C, while lactic acid was the main product at high temperature. This suggested that low temperature was not suitable for the retro-aldol reaction. Although lactic acid was the main product at high temperature, the selectivity of lactic acid still low. This due to the unknown peaks from HPLC results which cannot indicate that they were intermediates or by-products. Moreover, it can be suggested that the intermediates from fructose were adsorbed on the catalyst surface, making a decrease of selectivity of all products.

The selectivity of lactic acid from NaOH has a different trend with the metal oxide catalysts. The selectivity of lactic acid from the homogeneous catalyst (NaOH) decreased when increasing the reaction temperature, while the selectivity of lactic acid from heterogeneous catalysts increased. It may be due to the decomposition of

lactic acid to smaller carbon molecules such as acetic acid, etc. when the reaction was performed at high temperatures by NaOH. In case of metal oxide catalysts, the selectivity of lactic acid increased when increasing the reaction temperature. The changing in reaction temperature reflected the properties of water, which were the media of reaction. When the reaction temperature increased, the concentration of H^+ and OH^- in water also increased. A high concentration of H^+ and OH^- cases more chance in the adsorption of OH^- on the surface of solid catalyst, which increases the amount of basicity making higher lactic acid production. The selectivity of lactic acid was shown in descending order as ZnCTAB/MgO, NiCTAB/MgO, CuCTAB/MgO, and CoCTAB/MgO, respectively. The ZnCTAB/MgO gave the highest selectivity of lactic acid of 12% at 140°C. From previous studies, the role of catalyst in lactic acid production was reported by the attacked on the carbonyl carbon of intermediate from 2 ways including the hydroxyl group from alkaline solution and oxygen atom from metal oxide (Scheme 2.4). From the XRD patterns of used catalysts (Figure 4.2), it can be suggested that the role of CuCTAB/MgO and CoCTAB/MgO in lactic acid production was the use of oxygen atoms from metal oxide, while the NiCTAB/MgO and ZnCTAB/MgO used the hydroxyl group which formed at the catalyst surface. When considering the results of selectivity of lactic acid with the basicity from acid titration, it found that the trend of selectivity of lactic acid related to the amounts of basicity from acid titration accepted the CuCTAB/MgO. The selectivity of lactic acid from CuCTAB/MgO was lower than NiCTAB/MgO, but the basicity of fresh CuCTAB/MgO was higher. This suggested that the reducing of CuO to Cu₂O and Cu species during the reaction making less contact of the hydroxyl group at the surface of the catalyst, which was confirmed by the acid titration result of used catalyst. From the result of basicity and selectivity of lactic acid can be concluded that the role of basicity on the catalyst surface is more important than the binding oxygen atom from metal oxide and the basicity in the solution media.

4.2 Effects of the amounts of metal oxide loading on MgO catalysts on the lactic acid production from glucose

4.2.1 The physical and chemical properties of catalysts

4.2.1.1 X-Ray Diffraction (XRD).

When the metal content of catalysts increased, the XRD pattern of fresh and first used of catalysts with metal loading at 5 mmol/g-cat for lactic acid synthesis at 110°C, 1 h are shown in Figure 4.8 and 4.9, respectively.

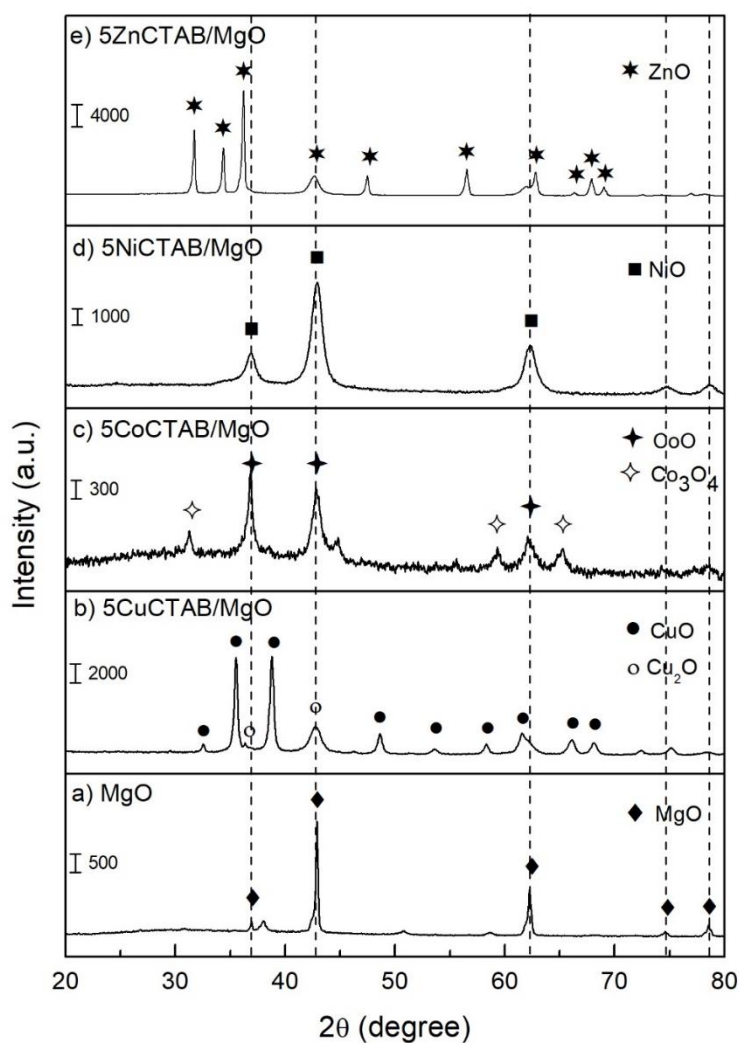


Figure 4.8 XRD patterns of fresh metal oxide supported on MgO catalysts with metal loading at 5 mmol/g-cat

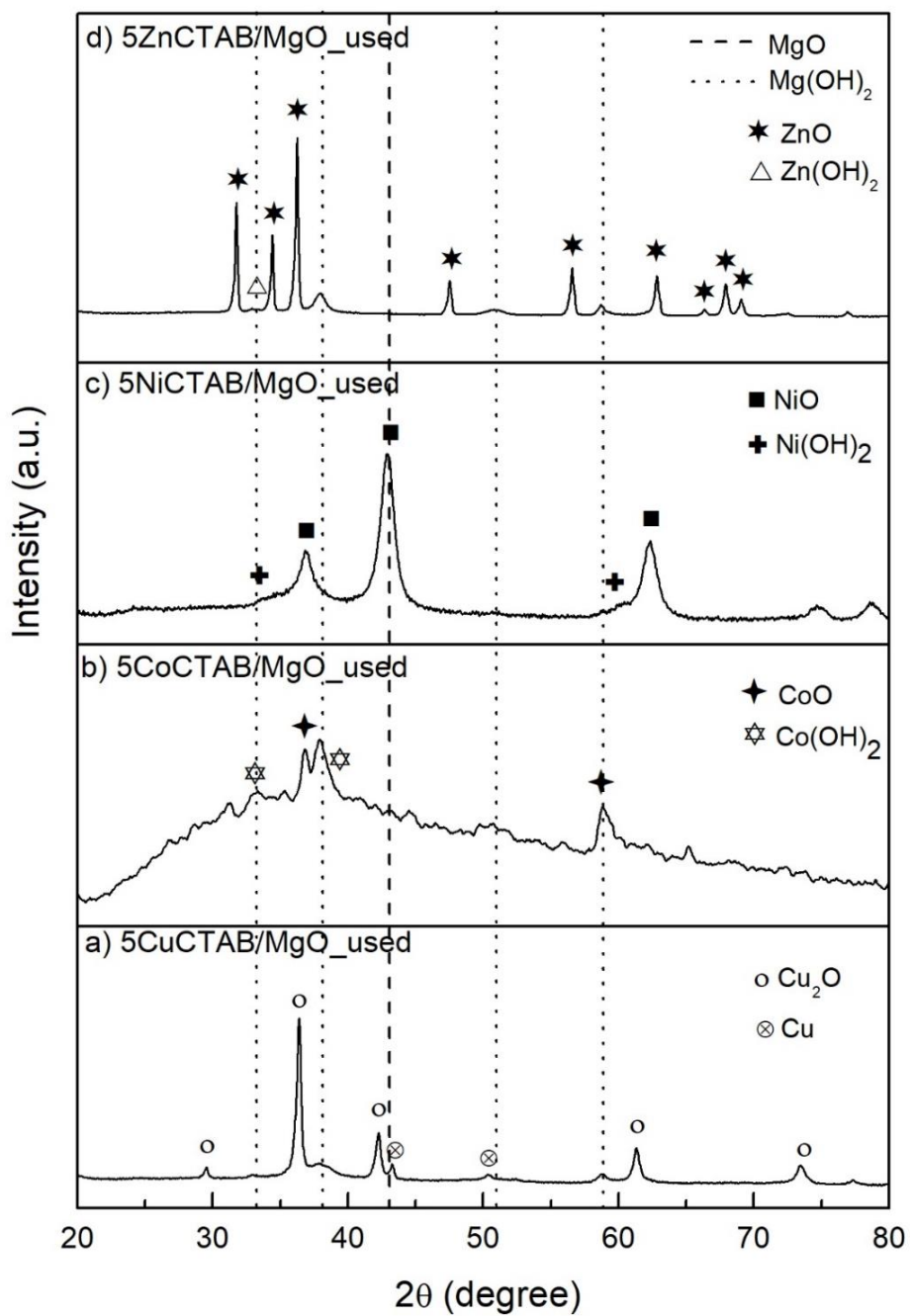


Figure 4.9 XRD patterns of used metal oxide supported on MgO catalysts with metal loading at 5 mmol/g-cat in the lactic acid synthesis from glucose at 110°C for 1 h

The XRD patterns of all fresh and used catalysts with metal loading at 5 mmol/g-cat has a similar trend with the metal loading at 1.5 mmol/g-cat. All fresh catalysts showed the phase of metal oxide with no impurities, while used catalyst exhibited metal hydroxide. The CuCTAB/MgO showed peaks of reduced metal (Cu_2O and Cu). The peak of Co_3O_4 disappeared from CoCTAB/MgO. These results confirmed the role of CuCTAB/MgO and CoCTAB/MgO catalysts for lactic production in term of oxygen usage from the metal oxide, while the others used hydroxyl ion which formed on the surface of the catalyst, as mentioned above.

4.2.1.2 Acid titration

The basicity of catalysts with various metal loading are shown in Table 4.5. The catalysts with 1.5 and 5 mmol metal/g-cat showed a similar trend with a descending order as ZnCTAB/MgO, CuCTAB/MgO, NiCTAB/MgO, and CoCTAB/MgO. While only 10 mmol/g-cat of CoCTAB/MgO catalyst has basicity on the catalyst surface.

Table 4.6 Amount of basicity of fresh various metal loading on MgO catalyst which was calculated from acid titration technique

Catalyst	Acid titration (mmol/g-cat)		
	1.5mmol/gcat	5mmol/gcat	10mmol/gcat
CuCTAB/MgO	3.8	3.6	-
CoCTAB/MgO	1.9	2.5	2.1
NiCTAB/MgO	2.6	3.0	-
ZnCTAB/MgO	4.8	4.9	-

4.2.1.3 Inductively Coupled Plasma-Atomic Emission Spectroscopy (ICP-AES)

The amounts of metal leaching from catalysts with metal loading at 5 and 10 mmol/g-cat after used in the reaction at 110°C and 140°C are shown in Table 4.6. The leachates of metal were increasing as increased metal loading.

Table 4.7 Amounts of metal leaching from lactic acid production from glucose by using catalysts at various metal loading

Catalyst	Metal content (mmol/g-cat)	Temperature (°C)	Amount of leaching (μmol)		
			Metal	Mg	SUM
CuCTAB/MgO	5	110	8.3	254.8	263.2
CoCTAB/MgO	5	110	21.9	215.5	237.4
NiCTAB/MgO	5	110	22.8	256.4	279.2
ZnCTAB/MgO	5	110	23.7	250.2	274.0
CuCTAB/MgO	10	110	24.9	5.5	30.5
CoCTAB/MgO	10	110	158.6	70.7	229.2
NiCTAB/MgO	10	110	26.3	9.0	35.3
ZnCTAB/MgO	10	110	24.7	1.7	26.5
CuCTAB/MgO	10	140	123.9	6.3	130.3
CoCTAB/MgO	10	140	922.9	283.4	1206.3
NiCTAB/MgO	10	140	178.1	17.4	195.5
ZnCTAB/MgO	10	140	143.5	1.4	144.9

4.2.2 Catalytic performance for lactic acid production from glucose

The glucose conversion and selectivity of lactic acid from metal oxide supported on MgO catalysts with various metal loading at 110°C are shown in Figure 4.10 and 4.11, respectively.

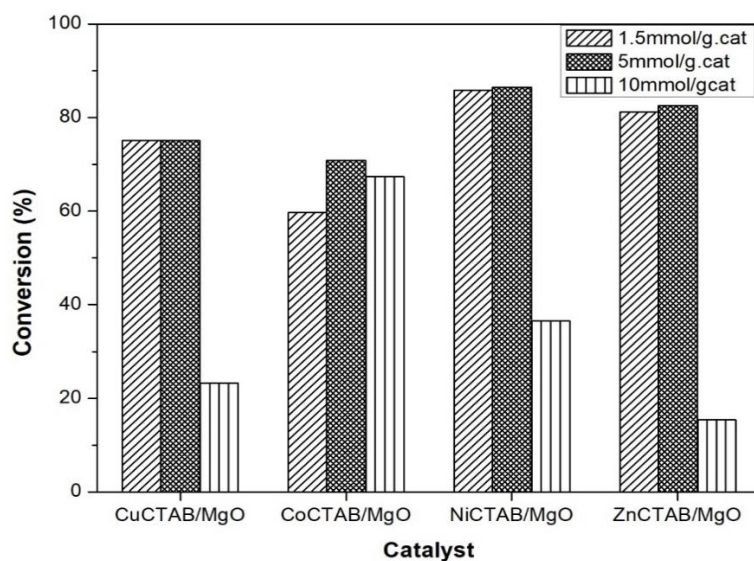


Figure 4.10 Catalytic activity of various metal loading on MgO catalysts at 110°C

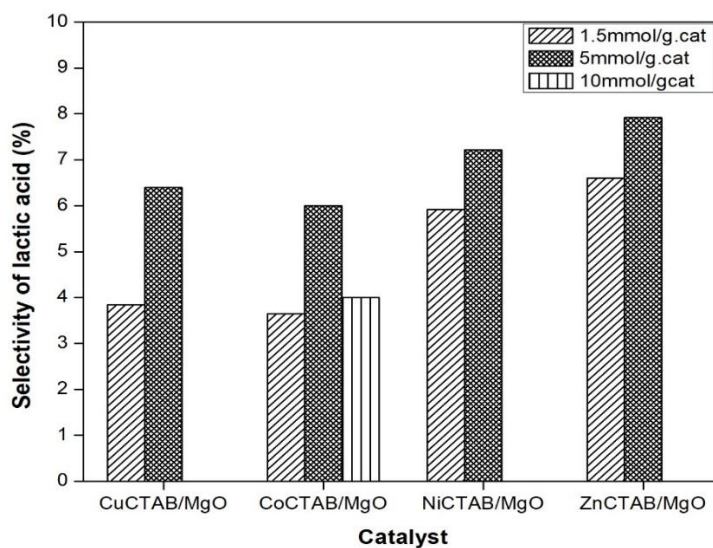


Figure 4.11 Selectivity of lactic acid of various metal loading on MgO catalysts at 110°C

When increased the amounts of metal loading from 1.5 to 5 mmol/g-cat, the conversion of CoCTAB/MgO increased, while the others have a smaller change. This results related to the amounts of metal leachate from the ICP technique. When further increasing the amounts of metal loading to 10 mmol/g-cat, the conversion of all catalysts decreased.

In terms of the selectivity of lactic acid, all catalysts have a similar trend which the selectivity of lactic acid increased as the increasing of the amount of metal loading from 1.5 to 5 mmol/g-cat. The high concentration of metal loading caused more chance in the adsorption of pyruvaldehyde (intermediate) to the surface of the catalyst, making more lactic acid production. The selectivity of lactic acid showed in descending order as ZnCTAB/MgO, NiCTAB/MgO, CuCTAB/MgO, and CoCTAB/MgO respectively which consistent with the amount of basicity from acid titration (Table 4.5). On the other hand, further loading metal to 10 mmol/g-cat, only CoCTAB/MgO showed the lactic acid produced according to the observed basicity on the surface of CoCTAB/MgO catalyst. This indicated that the basicity of the catalyst surface very affected to lactic acid production compared with the basicity in the solution.

Various metal content on MgO catalysts was performed at 140°C to confirm the effect of basicity of the catalyst surface on the selectivity of lactic acid and the effect of temperature on lactic acid production. The results are shown in Figure. 4.12-4.13.

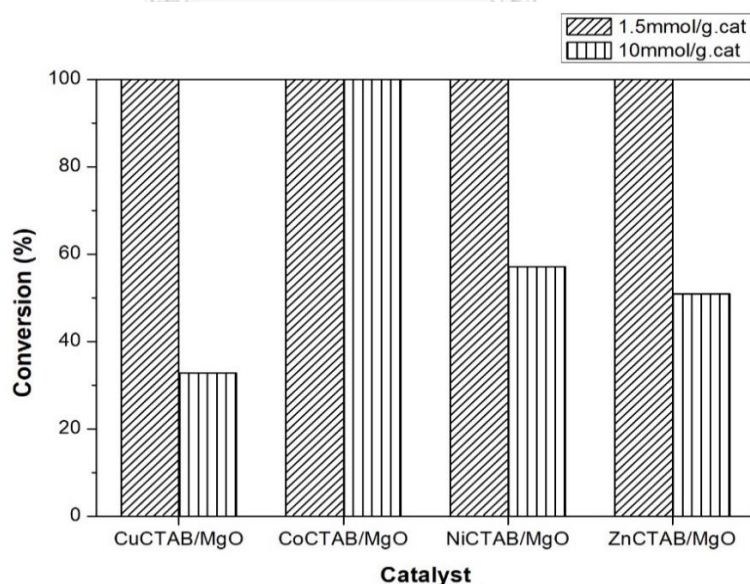


Figure 4.12 Catalytic activity of various metal loading on MgO catalyst at 140°C

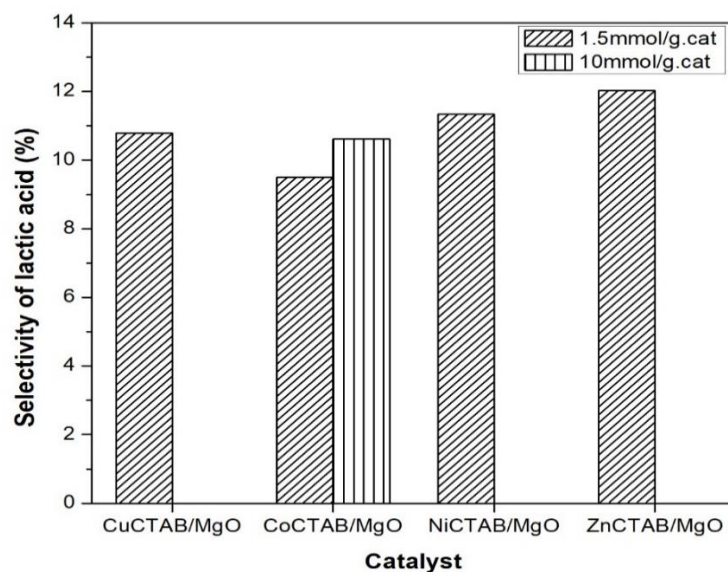


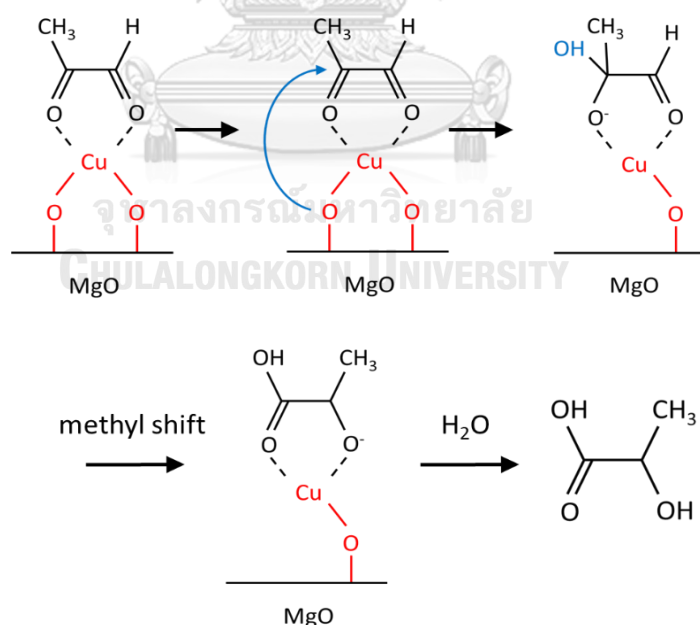
Figure 4.13 Selectivity of lactic acid of various metal loading on MgO catalyst at 140°C

When the reaction performed at 140°C, the catalysts with metal loading at 10 mmol/g-cat gave glucose conversion of 100% from CoCTAB/MgO, which related to a large amount of metal leaching from the CoCTAB/MgO catalyst. For lactic acid production, only CoCTAB/MgO showed the selectivity of lactic acid. This result confirmed the role of basicity of solid catalyst for selectivity of lactic acid. In term of reaction temperature, the CuCTAB/MgO, NiCTAB/MgO, and ZnCTAB/MgO catalysts with metal loading at 10 mmol/g-cat were not observed lactic acid production at 110°C and 140°C. It indicated that the reaction temperature has no affected to the selectivity of lactic acid if the catalyst showed no basicity of solid catalyst surface.

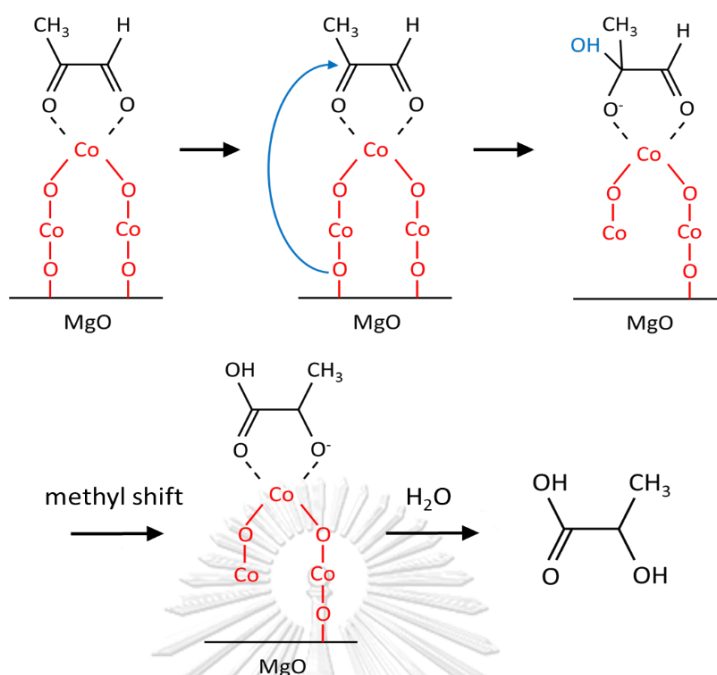
4.3 Proposed mechanism

The mechanistic pathways for lactic acid production from glucose beginning from the isomerization of glucose to fructose, followed by the retro-aldol fragmentation to glyceraldehyde and dihydroxyacetone. Then, the glyceraldehyde dehydrated to pyruvaldehyde, which was adsorbed onto the catalyst surface, making the catalyst-pyruvaldehyde complex molecule. After that, this intermediate

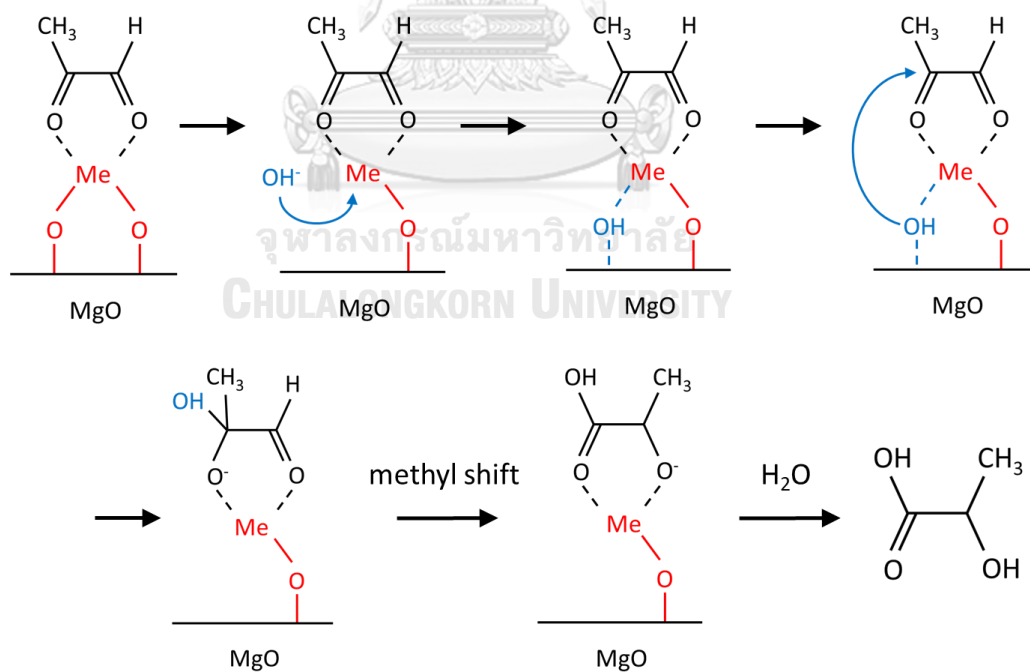
transferred into lactic acid via a methyl shift reaction (Scheme 2.4) [11]. Based on the previous researches and results in this study, the step of the transformation from the catalyst-pyruvaldehyde complex molecule to lactic acid by using CuCTAB/MgO, CoCTAB/MgO, NiCTAB/MgO, and ZnCTAB/MgO catalyst was different. The CuCTAB/MgO and CoCTAB/MgO have 2 pathways, which the oxygen atom of metal oxide from the catalyst attacked the carbonyl carbon of pyruvaldehyde making a reduced metal species (from CuO to Cu₂O, Cu and Co₃O₄ to CoO) and used the hydroxyl group which form by the chemisorption of water molecule at the catalyst surface. On the other hand, the NiCTAB/MgO and ZnCTAB/MgO have 1 pathway, which the usage of the hydroxyl group at the catalyst surface. The proposed mechanistic pathway of CuCTAB/MgO and CoCTAB/MgO in term of the usage of oxygen atom from metal oxide are shown as Scheme 4.1 and 4.2, while the mechanistic pathway of all catalysts in term of the usage of the hydroxyl group at the catalyst surface are shown as Scheme 4.3.



Scheme 4.1 Proposed reaction pathway for the usage of oxygen atom of CuCTAB/MgO catalyst [11]



Scheme 4.2 Proposed reaction pathway for the usage of oxygen atom of CoCTAB/MgO catalyst



Scheme 4.3 Proposed reaction pathway for the usage of the hydroxyl group at the catalyst surface of metal oxide supported on MgO catalysts
(The Me represent the various metal species: Cu, Co, Ni, and Zn)

CHAPTER V

CONCLUSIONS AND RECOMMENDATIONS

5.1 Conclusions

In this research, the effects of various metal oxide (Cu, Co, Ni, and Zn) supported on MgO catalysts by using CTAB as the capping agent and the effects of the amounts of metal loading (1.5, 5, and 10 mmol/g-cat) on glucose conversion and selectivity of lactic acid were investigated. The reaction was performed in an alkali additive-free environment.

The XRD patterns of fresh and used catalysts indicated the differences in the role of various metal oxide supported on MgO catalysts for lactic acid production. For the CuCTAB/MgO and CoCTAB/MgO can use the oxygen atom from metal oxide making the reduced metal species on the surface of catalyst or the hydroxyl group which form by the chemisorption of a water molecule at the catalyst surface. While the NiCTAB/MgO and ZnCTAB/MgO only used the hydroxyl group at the catalyst surface.

For the catalyst with metal loading at 1.5 mmol/g-cat, the activity of all catalysts at the reaction temperature below 120°C have a similar trend, the pure MgO gave the highest glucose conversion of 89.2% at 110°C with the highest amounts of Mg leaching and basicity of the leachate solution. Additionally, the trend of glucose conversion from various metal oxide supported on MgO catalysts were related to the amounts of metal leaching from the ICP result, which indicated that the metal ion and basicity from metal hydroxide in the solution has very affected to the glucose conversion. In case of selectivity of lactic acid, the ZnCTAB/MgO gave the highest selectivity of 12% at 140°C. The selectivity of lactic acid consistent with the basicity from acid titration suggested that the basicity of solid catalyst surface very

affected to the selectivity of lactic acid. This suggestion was confirmed by the results of the catalyst with the metal content of 5 and 10 mmol/g-cat.

5.2 Recommendations

1. The reaction time should be varied to investigate the optimum condition for lactic acid production from glucose.
2. The stability test of the catalyst should be provided.
3. The other products should be investigated.



REFERENCES

- [1] Gao, C., Ma, C., and Xu, P. Biotechnological routes based on lactic acid production from biomass. Biotechnology Advances 29(6) (2011): 930-939.
- [2] Si, W.-J., Yang, L., Weng, Y.-X., Zhu, J., and Zeng, J.-B. Poly(lactic acid)/biobased polyurethane blends with balanced mechanical strength and toughness. Polymer Testing 69 (2018): 9-15.
- [3] Jem, K.J., van der Pol, J.F., and de Vos, S. Microbial Lactic Acid, Its Polymer Poly(lactic acid), and Their Industrial Applications. in Chen, G.G.-Q. (ed.) Plastics from Bacteria: Natural Functions and Applications, pp. 323-346. Berlin, Heidelberg: Springer Berlin Heidelberg, 2010.
- [4] Limited, C.R. Lactic Acid Market By Application (Food And Beverages, Pharmaceuticals, Industrial Applications, Personal Care Products) - Growth, Share, Opportunities & Competitive Analysis, 2015 - 2022 2016. Available from: <https://www.credenceresearch.com/report/lactic-acid-market>
- [5] Corbion. Corbion starts construction of 75kTpa PLA bioplastics plant 2016. Available from: <http://www.corbion.com/media/press-releases?newsId=2056582> [14 November]
- [6] Lactic Acid Market Analysis By Application (Industrial, F&B, Pharmaceuticals, Personal Care) & Polylactic Acid (PLA) Market Analysis By Application (Packaging, Agriculture, Transport, Electronics, Textiles), And Segment Forecasts, 2018 - 2025 2017. Available from: <https://www.grandviewresearch.com/industry-analysis/lactic-acid-and-poly-lactic-acid-market>
- [7] Jin, F. Application of hydrothermal reactions to biomass conversion. Green Chemistry and Sustainable Technology, ed. He, L.-N., Rogers, R.D., Su, D., Tundo, P., and Zhang, Z.C. London: Springer-Verlag Berlin Heidelberg, 2014.
- [8] Li, S., Deng, W., Li, Y., Zhang, Q., and Wang, Y. Catalytic conversion of cellulose-based biomass and glycerol to lactic acid. Journal of Energy Chemistry (2018).
- [9] Yan, X., Jin, F., Tohji, K., Moriya, T., and Enomoto, H. Production of lactic acid from glucose by alkaline hydrothermal reaction. Journal of Materials Science

- 42(24) (2007): 9995-9999.
- [10] Huo, Z., Fang, Y., Ren, D., Zhang, S., Yao, G., Zeng, X., et al. Selective Conversion of Glucose into Lactic Acid with Transition Metal Ions in Diluted Aqueous NaOH Solution. ACS Sustainable Chemistry & Engineering 2(12) (2014): 2765-2771.
- [11] Choudhary, H., Nishimura, S., and Ebitani, K. Synthesis of high-value organic acids from sugars promoted by hydrothermally loaded Cu oxide species on magnesia. Applied Catalysis B: Environmental 162 (2015): 1-10.
- [12] Cleaves, H.J. Lactic Acid. in Gargaud, M., et al. (eds.), Encyclopedia of Astrobiology, pp. 1355-1356. Berlin, Heidelberg: Springer Berlin Heidelberg, 2015.
- [13] Ren, J. Lactic Acid. in Ren, J. (ed.) Biodegradable Poly(Lactic Acid): Synthesis, Modification, Processing and Applications, pp. 4-14. Berlin, Heidelberg: Springer Berlin Heidelberg, 2010.
- [14] Database, P.C. Lactic Acid. National Center for Biotechnology Information.
- [15] Dusselier, M., Van Wouwe, P., Dewaele, A., Makshina, E., and Sels, B.F. Lactic acid as a platform chemical in the biobased economy: the role of chemocatalysis. Energy & Environmental Science 6(5) (2013): 1415.
- [16] Global Lactic Acid and Polylactic Acid Market 2018. Available from: <https://www.transparencymarketresearch.com/pressrelease/lactic-poly-lactic-acid.htm>
- [17] Sad, M.E., González Peña, L.F., Padró, C.L., and Apesteguía, C.R. Selective synthesis of acetaldehyde from lactic acid on acid zeolites. Catalysis Today 302 (2018): 203-209.
- [18] Vandenberghe, L.P.S., Karp, S.G., de Oliveira, P.Z., de Carvalho, J.C., Rodrigues, C., and Soccol, C.R. Chapter 18 - Solid-State Fermentation for the Production of Organic Acids. in Pandey, A., Larroche, C., and Soccol, C.R. (eds.), Current Developments in Biotechnology and Bioengineering, pp. 415-434: Elsevier, 2018.
- [19] Rogers, T. Everything You Need To Know About Polylactic Acid (PLA) 2015. Available from: <https://www.creativemechanisms.com/blog/learn-about-poly-lactic-acid-pla-prototypes>
- [20] World, G. What Are Corn Starch Biocompostables aka PLA Plastics? Available from: <http://www.greenworld365.com/what-are-corn-starch-biocompostables->

aka-pla-plastics/

- [21] Mäki-Arvela, P., Simakova, I.L., Salmi, T., and Murzin, D.Y. Production of Lactic Acid/Lactates from Biomass and Their Catalytic Transformations to Commodities. Chemical Reviews 114(3) (2014): 1909-1971.
- [22] Ameen, S.M. and Caruso, G. Chemistry of Lactic Acid. in Ameen, S.M. and Caruso, G. (eds.), Lactic Acid in the Food Industry, pp. 7-17. Cham: Springer International Publishing, 2017.
- [23] Ghaffar, T., Irshad, M., Anwar, Z., Aqil, T., Zulifqar, Z., Tariq, A., et al. Recent trends in lactic acid biotechnology: A brief review on production to purification. Journal of Radiation Research and Applied Sciences 7(2) (2014): 222-229.
- [24] Xu, Q.-T., Li, J.-C., Xue, H.-G., and Guo, S.-P. Binary iron sulfides as anode materials for rechargeable batteries: Crystal structures, syntheses, and electrochemical performance. Journal of Power Sources 379 (2018): 41-52.
- [25] Wang, Y., Jin, F., Sasaki, M., Wahyudiono, Wang, F., Jing, Z., et al. Selective conversion of glucose into lactic acid and acetic acid with copper oxide under hydrothermal conditions. AIChE Journal 59(6) (2013): 2096-2104.
- [26] Adam, Y.S., Fang, Y., Huo, Z., Zeng, X., Jing, Z., and Jin, F. Production of carboxylic acids from glucose with metal oxides under hydrothermal conditions. Research on Chemical Intermediates 41(5) (2013): 3201-3211.
- [27] Xue, Y., Jin, F., and Yoshikawa, K. Hydrothermal Lactic Acid Production from Glucose over Feldspars as Solid Base Catalysts in Water. Energy Procedia 61 (2014): 2474-2477.
- [28] Duo, J., Zhang, Z., Yao, G., Huo, Z., and Jin, F. Hydrothermal conversion of glucose into lactic acid with sodium silicate as a base catalyst. Catalysis Today 263 (2016): 112-116.
- [29] Gao, X., Zhong, H., Yao, G., Guo, W., and Jin, F. Hydrothermal conversion of glucose into organic acids with bentonite as a solid-base catalyst. Catalysis Today 274 (2016): 49-54.
- [30] Yang, X., Yang, L., Fan, W., and Lin, H. Effect of redox properties of LaCoO₃ perovskite catalyst on production of lactic acid from cellulosic biomass. Catalysis Today 269 (2016): 56-64.

- [31] Li, L., Shen, F., Smith, R.L., and Qi, X. Quantitative chemocatalytic production of lactic acid from glucose under anaerobic conditions at room temperature. Green Chemistry 19(1) (2017): 76-81.
- [32] Onda, A., Ochi, T., Kajiyoshi, K., and Yanagisawa, K. A new chemical process for catalytic conversion of d-glucose into lactic acid and gluconic acid. Applied Catalysis A: General 343(1-2) (2008): 49-54.
- [33] Onda, A., Ochi, T., Kajiyoshi, K., and Yanagisawa, K. Lactic acid production from glucose over activated hydrotalcites as solid base catalysts in water. Catalysis Communications 9(6) (2008): 1050-1053.
- [34] Hou, G.-h. and Yan, L.-f. Synthesis of Pb(OH)₂/rGO Catalyst for Conversion of Sugar to Lactic Acid in Water. Chinese Journal of Chemical Physics 28(4) (2015): 533-538.
- [35] Herceg, Z. and Murr, R. Chapter 3 - Mechanisms of Histone Modifications. in Tollefsbol, T. (ed.) Handbook of Epigenetics, pp. 25-45. San Diego: Academic Press, 2011.
- [36] Shapley, P. Biosynthesis of Fat 2012. Available from: <http://butane.chem.uiuc.edu/pshapley/GenChem2/B11/2.html>
- [37] Zhang, S.-L. and Deng, Z.-Q. Copper-catalyzed retro-aldol reaction of β -hydroxy ketones or nitriles with aldehydes: chemo- and stereoselective access to (E)-enones and (E)-acrylonitriles. Organic & Biomolecular Chemistry 14(30) (2016): 7282-7294.
- [38] Zak, D. a typical aldol reaction From Eugene's version 2006. Available from: https://en.wikipedia.org/wiki/Aldol_reaction
- [39] Abd.Rahman, N., Hasan, M., Hussain, M., and Jahim, J. Determination of Glucose and Fructose from Glucose Isomerization Process by High performance Liquid Chromatography with UV Detection. Modern applied science 2 (2009).
- [40] Mastuli, M.S., Kamarulzaman, N., Kasim, M.F., Sivasangar, S., Saiman, M.I., and Taufiq-Yap, Y.H. Catalytic gasification of oil palm frond biomass in supercritical water using MgO supported Ni, Cu and Zn oxides as catalysts for hydrogen production. International Journal of Hydrogen Energy 42(16) (2017): 11215-

11228.

- [41] Li, H.-j., Zheng, L., Zhao, T.-q., and Xu, X.-f. Effect of preparation parameters on the catalytic performance of hydrothermally synthesized Co₃O₄ in the decomposition of N₂O. Journal of Fuel Chemistry and Technology 46(6) (2018): 717-724.
- [42] Liu, M., Li, Y., Wang, K., Luo, Y., Hou, S., Wang, P., et al. Solvent-controlled synthesis of mesoporous CoO with different morphologies as binder-free anodes for lithium-ion batteries. Ceramics International 44(16) (2018): 19631-19638.
- [43] Sangeeta, M., Karthik, K.V., Ravishankar, R., Anantharaju, K.S., Nagabhushana, H., Jeetendra, K., et al. Synthesis of ZnO, MgO and ZnO/MgO by Solution Combustion Method: Characterization and Photocatalytic Studies. Materials Today: Proceedings 4(11, Part 3) (2017): 11791-11798.
- [44] Puriwat, J., Chaitree, W., Suriye, K., Dokjampa, S., Praserttham, P., and Panpranot, J. Elucidation of the basicity dependence of 1-butene isomerization on MgO/Mg(OH)₂ catalysts. Catalysis Communications 12(2) (2010): 80-85.
- [45] YongKang Chen, Z.A.a.M.C. Competition Mechanism Study of Mg+H₂O and MgO+H₂O Reaction. IOP Conference Series: Materials Science and Engineering 394 (2018).
- [46] Fan, Y., Wang, L., Huang, W., Dong, Y., Ma, Z., Guo, W., et al. Co(OH)₂@Co electrode for efficient alkaline anode based on Co²⁺/Co⁰ redox mechanism. Energy Storage Materials (2018).
- [47] Dimitrios A. Giannakoudakis, T.J.B. Detoxification of Chemical Warfare Agents: From WWI to Multifunctional Nanocomposite Approaches. Springer, 2017.
- [48] Li, X., Ding, R., Shi, W., Xu, Q., Ying, D., Huang, Y., et al. Hierarchical porous Co(OH)F/Ni(OH)₂: A new hybrid for supercapacitors. Electrochimica Acta 265 (2018): 455-473.
- [49] Sengupta, G., Ahluwalia, H.S., Banerjee, S., and Sen, S.P. Chemisorption of water vapor on zinc oxide. Journal of Colloid and Interface Science 69(2) (1979): 217-224.
- [50] Zhao, W., Bajdich, M., Carey, S., Vojvodic, A., Nørskov, J.K., and Campbell, C.T. Water Dissociative Adsorption on NiO(111): Energetics and Structure of the

- Hydroxylated Surface. ACS Catalysis 6(11) (2016): 7377-7384.
- [51] Wu, M., Fu, Y., Zhan, W., Guo, Y., Guo, Y., Wang, Y., et al. Catalytic Performance of MgO-Supported Co Catalyst for the Liquid Phase Oxidation of Cyclohexane with Molecular Oxygen. Catalysts 7(5) (2017): 155.
- [52] Xu, S., Huang, C., Zhang, J., and Chen, B. Catalytic activity of Cu/MgO in liquid phase oxidation of cumene. Korean Journal of Chemical Engineering 26(6) (2009): 1568-1573.
- [53] Pandhare, N.N., Pudi, S.M., Biswas, P., and Sinha, S. Selective Hydrogenolysis of Glycerol to 1,2-Propanediol over Highly Active and Stable Cu/MgO Catalyst in the Vapor Phase. Organic Process Research & Development 20(6) (2016): 1059-1067.
- [54] Graça, I., Bacariza, M.C., and Chadwick, D. Glucose isomerisation into fructose over Mg-impregnated Na-zeolites: Influence of zeolite structure. Microporous and Mesoporous Materials 255 (2018): 130-139.
- [55] Wang, Y., Deng, W., Wang, B., Zhang, Q., Wan, X., Tang, Z., et al. Chemical synthesis of lactic acid from cellulose catalysed by lead(II) ions in water. Nat Commun 4 (2013): 2141.
- [56] Dewick, P.M. Essentials of Organic Chemistry.: For Students of Pharmacy, Medicinal Chemistry and Biological Chemistry. Wiley, 2013.



APPENDIX A

CALCULATION OF CATALYST PREPARATION

The hydrothermal synthesis of metal oxides supported on MgO catalyst using CTAB as the capping agent can be calculated as below

A.1 Calculation of metal loading and CTAB content

All catalysts were prepared by using metal and CTAB in the ratio of 1:1 and give

- A = The mmol of metal loading per gram catalyst
- B = The weight of catalyst required
- C = The ratio of mole of metal in precursor to mole of precursor
- MW_i = Molecular weight of i
- D = Purity of precursor

$$\text{Weight of metal precursor required} = \frac{A \times B \times MW_{\text{metal precursor}} \times C}{D}$$

$$\text{Weight of CTAB required} = A \times B \times MW_{\text{CTAB}}$$

$$\text{Weight of MgO required} = B - (A \times B \times MW_{\text{metal}})$$

A.2 Example calculation of CuCTAB/MgO catalyst with Cu loading in 1.5 mmol/g-cat

- Prepared catalyst 3 g
- The copper nitrate hexahydrate was used as precursor

$$\text{Weight of metal precursor required} = \frac{0.0015 \times 3 \times 241.6 \times 1}{0.98} = 1.11 \text{ g}$$

$$\text{Weight of CTAB required} = 0.0015 \times 3 \times 364.45 = 1.64 \text{ g}$$

$$\text{Weight of MgO required} = 3 - (0.0015 \times 3 \times 63.546) = 2.71 \text{ g}$$

APPENDIX B

CALCULATION OF TOTAL BASIC SITES OF CATALYST

The basicity properties on surface catalysts were characterized by CO₂-TPD technique which can be calculated from the CO₂-TPD profiles by following these steps.

B.1 Calibration curve between carbon dioxide content and area which obtained from the CO₂-TPD profiles

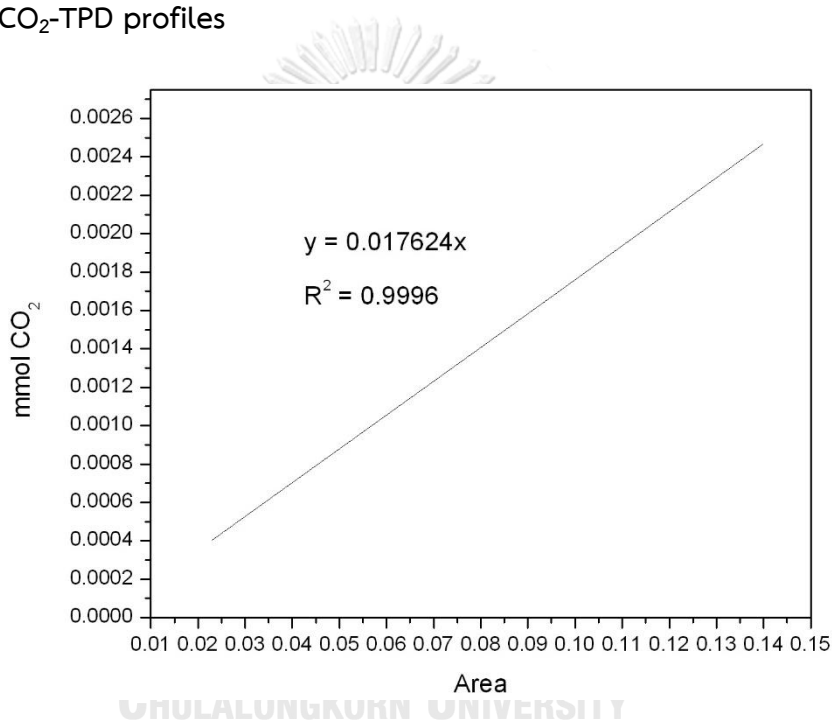


Figure B.1 The calibration curve of carbon dioxide obtained from Micromeritics 2750

B.2 The calculation of basicity from the CO₂-TPD profiles

Give

- A = The area of the CO₂-TPD profiles of each catalyst
- B = The amount of catalyst

$$\text{The basicity of catalyst (mmol CO}_2\text{/g.cat)} = \frac{0.017624 \times A}{B}$$

APPENDIX C
SEM IMAGES AND EDX MAPS OF METAL OXIDE SUPPORTED ON
MgO CATALYST

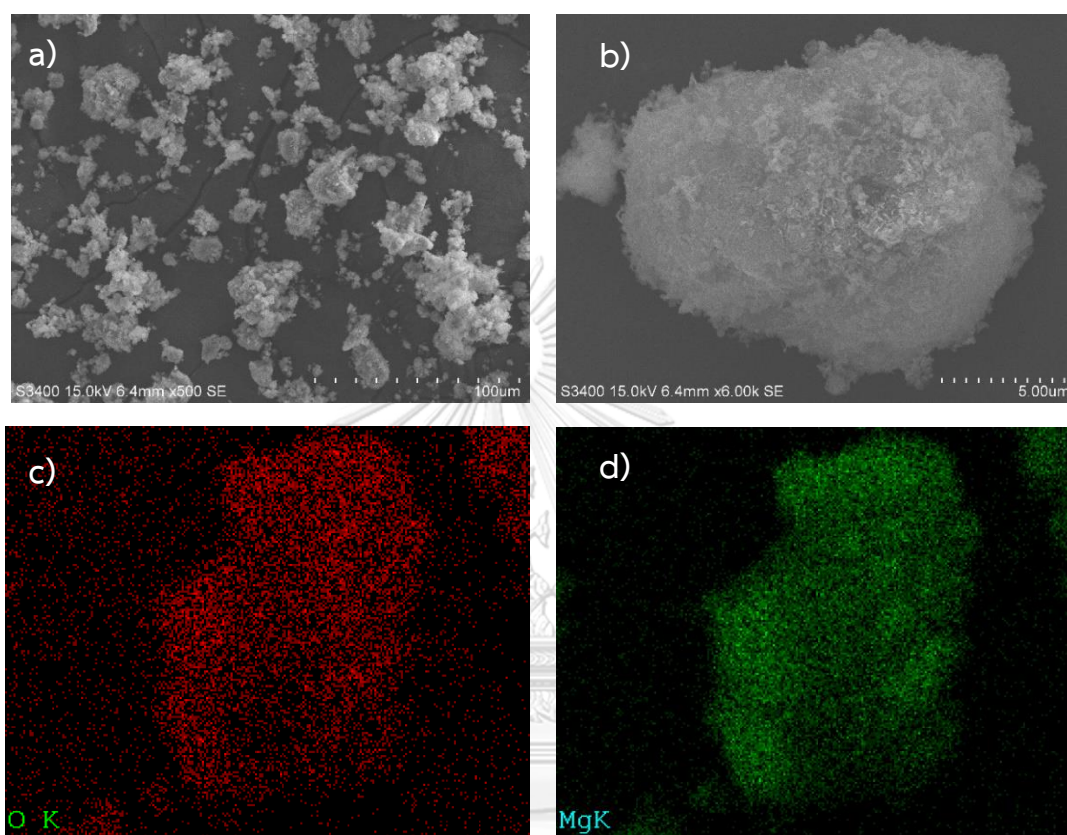


Figure C.1 SEM images at 500 and 6,000 magnification and EDX mapping of O and Mg for CuCTAB/MgO with Cu loading of 1.5 mmol/g-cat

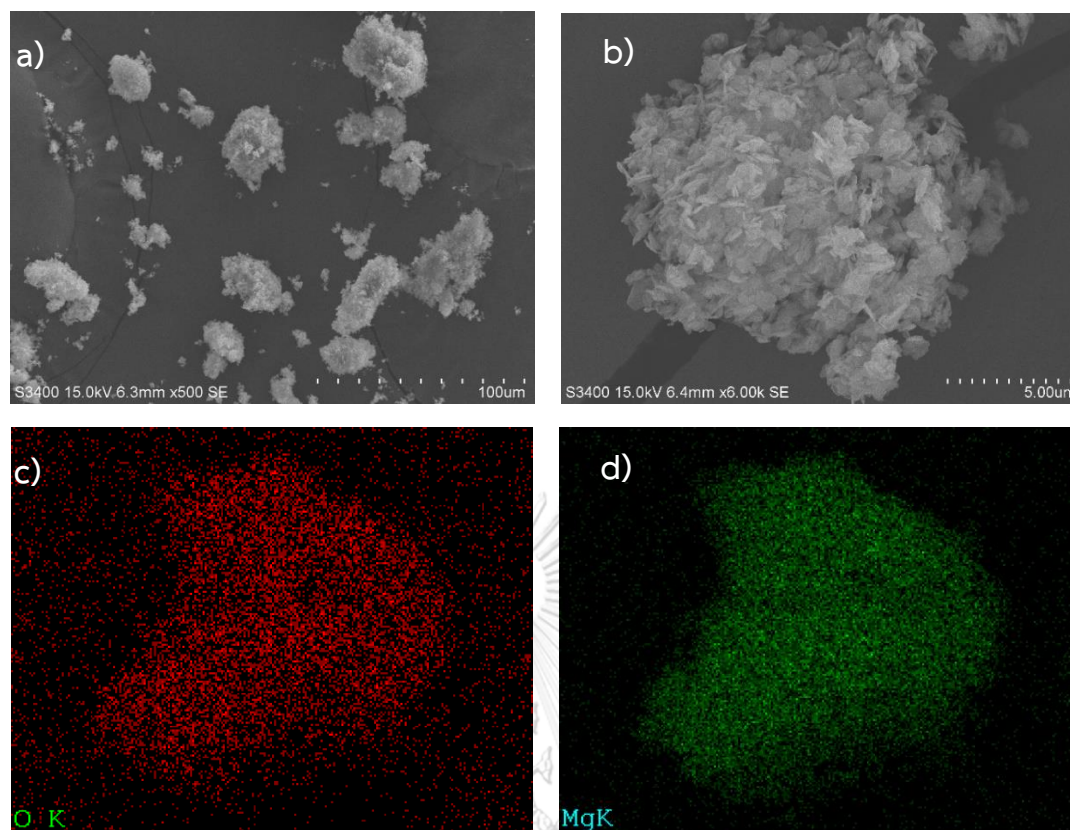


Figure C.2 SEM images at 500 and 6,000 magnification and EDX mapping of O and Mg for CoCTAB/MgO with Co loading of 1.5 mmol/g-cat

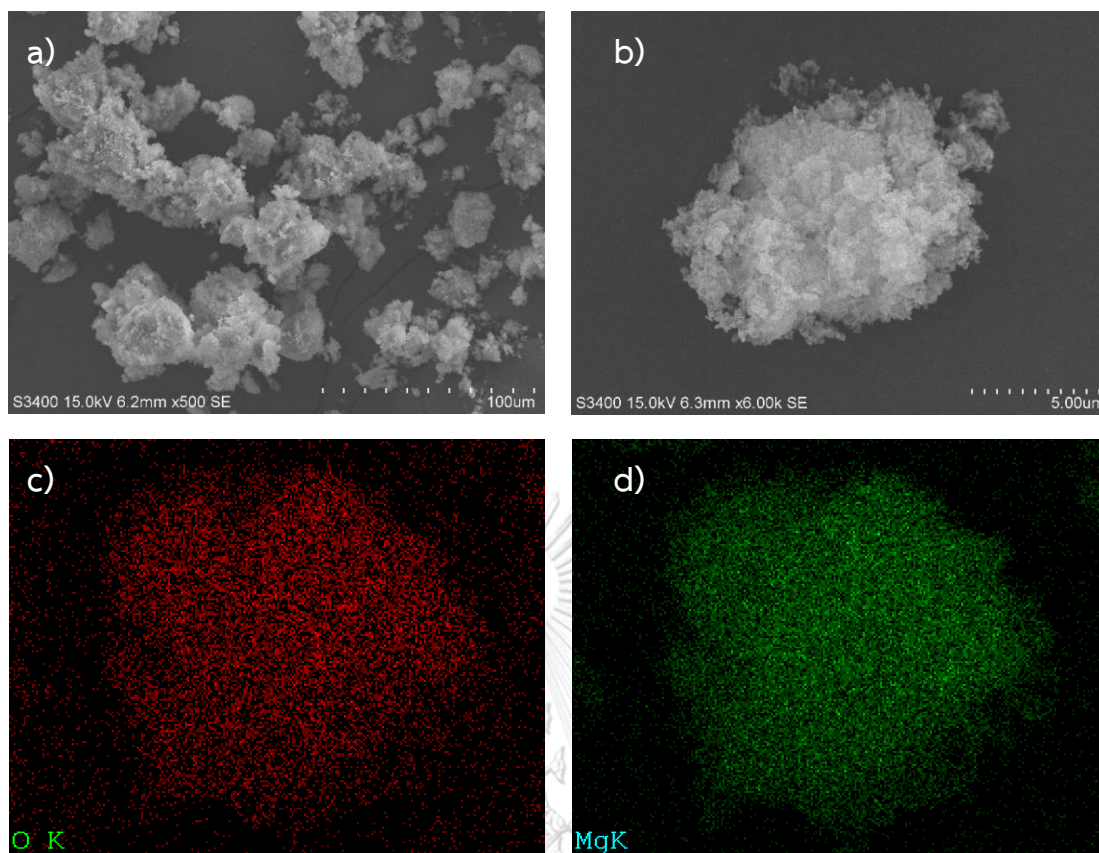


Figure C.3 SEM images at 500 and 6,000 magnification and EDX mapping of O and Mg for NiCTAB/MgO with Ni loading of 1.5 mmol/g-cat

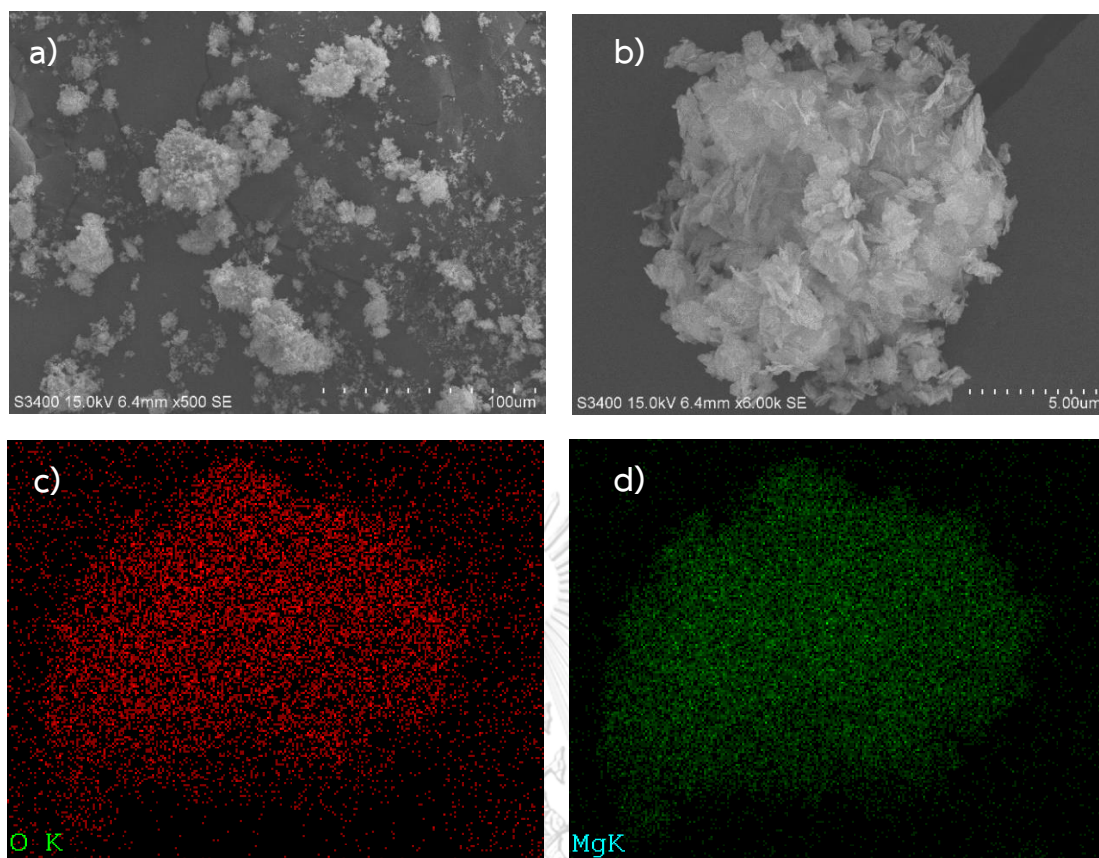


Figure C.4 SEM images at 500 and 6,000 magnification and EDX mapping of O and Mg for ZnCTAB/MgO with Zn loading of 1.5 mmol/g-cat

APPENDIX D

CALIBRATION CURVES OF REAGENTS

The conversion and selectivity of lactic acid production process from glucose was calculated from the calibration curves of each reagent which done from a high performance liquid chromatography (HPLC, Agilent LC 1100 equipped with UV-detector).

The reactant of this reaction is glucose and the main product is lactic acid. The intermediate is fructose. While by-products are formic acid and acetic acid.

The solution of standard reagents were injected into HPLC at different concentration. The peak area which analyzed from HPLC were plotted versus concentration of the sample to make the calibration curves. The calibration curves of each reagents are presented below.

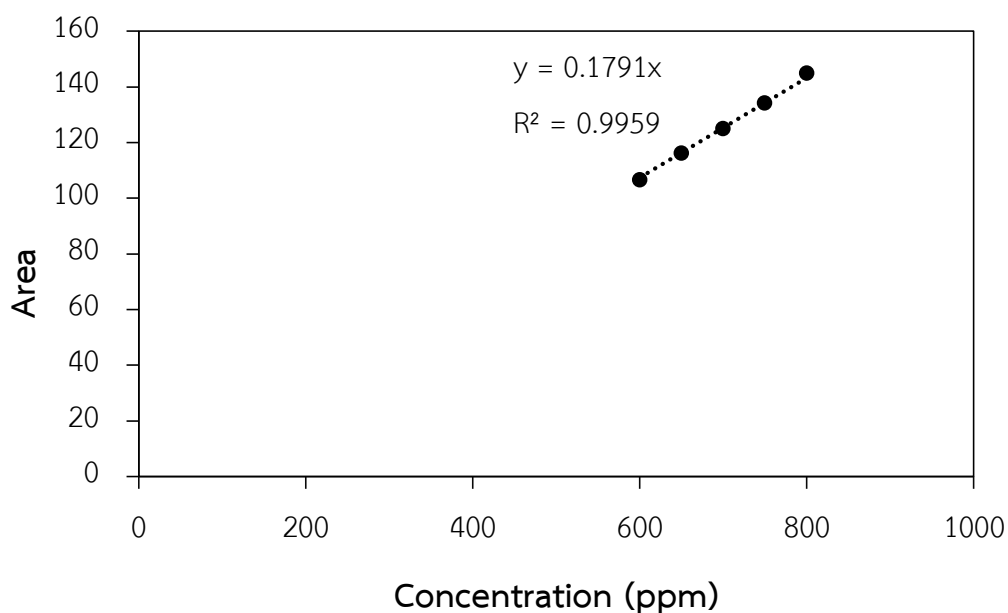


Figure D.1 Calibration curve of glucose

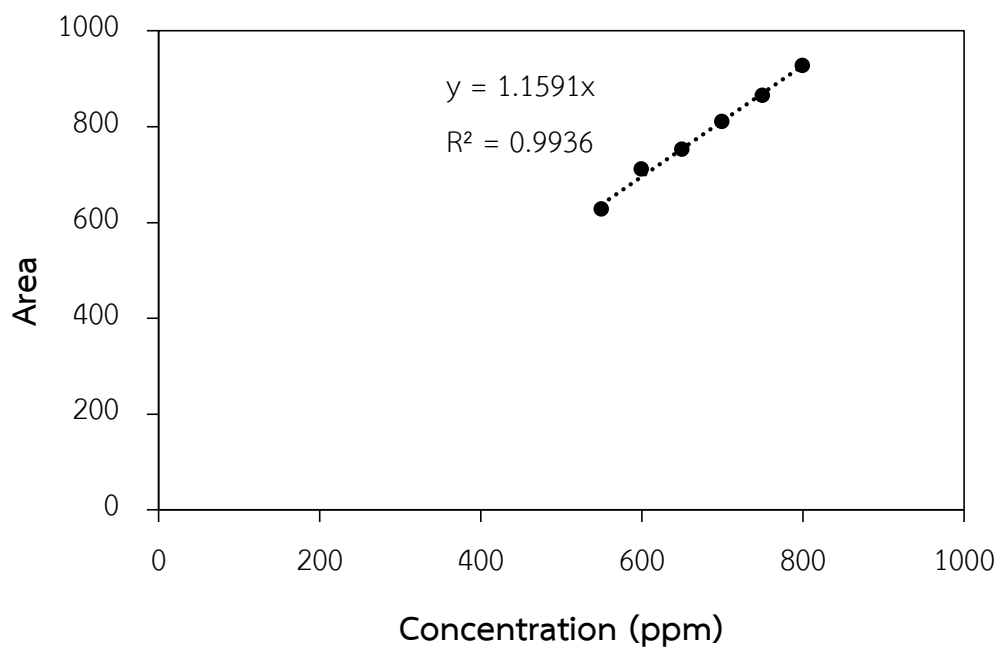


Figure D.2 Calibration curve of lactic acid

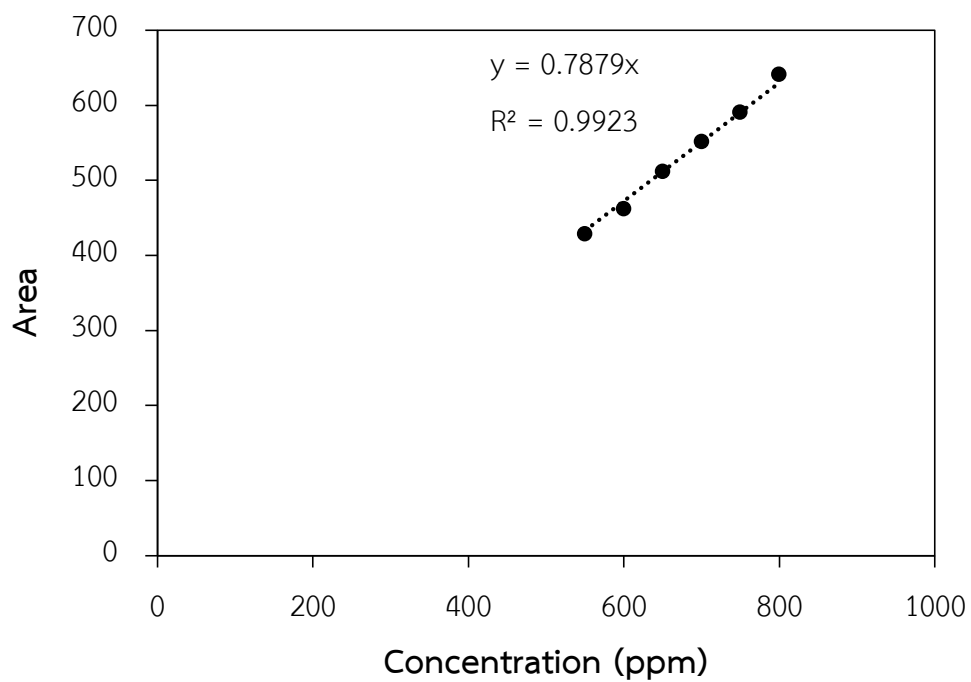


Figure D.3 Calibration curve of fructose

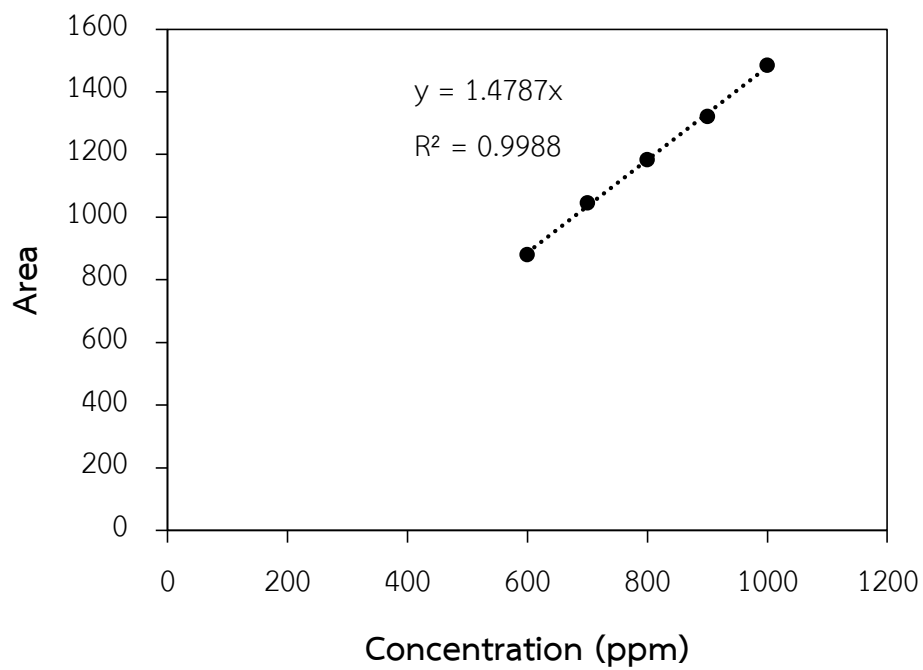


Figure D.4 Calibration curve of glyceraldehyde

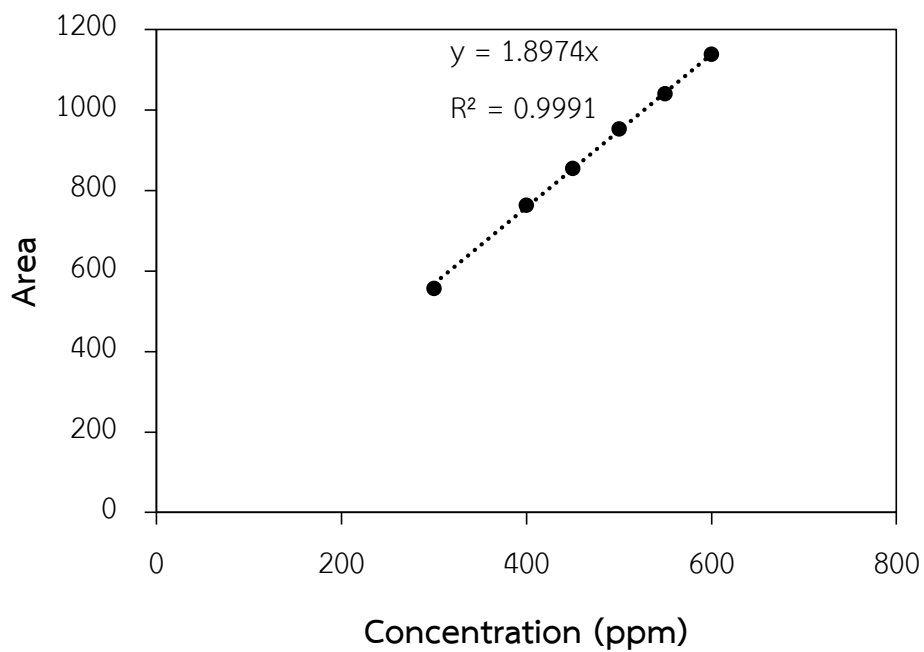


Figure D.5 Calibration curve of formic acid

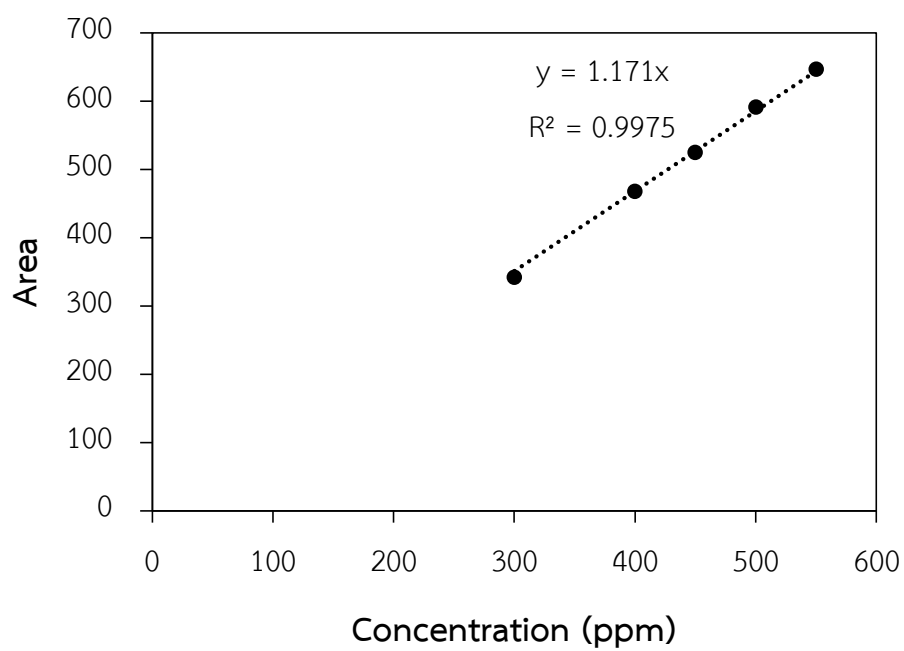


Figure D.6 Calibration curve of Acetic acid



APPENDIX E

THE DEGRADATION OF INTERMEDIATES AND LACTIC ACID TO BY-PRODUCTS

To investigate the effect of the degradation of intermediates and lactic acid to by-products, the lactic acid production from glucose process was performed at 1 and 2 hours by using ZnCTAB/MgO with metal loading of 1.5 mmol/g-cat as catalyst. The results are shown in Table E.1.

Table E.1 Effect of reaction time on lactic acid production from glucose by using ZnCTAB/MgO with metal loading of 1.5 mmol/g-cat

Reaction time (h)	Conversion (%)	Selectivity (%)						Ratio of the selectivity of Intermediates/ By-products	Ratio of the selectivity of Lactic acid/ By-products	
		Lactic acid	Intermediates		By-products					
			Fructose	Glyceraldehyde	SUM	Formic acid	Acetic acid			SUM
1	81.1	6.6	30.6	0.0	30.6	0.2	0.7	0.9	33.3	7.2
2	100.0	7.4	39.8	3.0	42.8	0.7	1.1	1.8	23.7	4.1

According to the results, It is likely that the differential of the ratio between the selectivity of intermediates to by-products at the reaction time at 1 and 2 hours is 9.6, which was more than the ratio between the selectivity of lactic acid to by-products (3.1). It is indicating that the by-products were generated by the decomposition of intermediates more than lactic acid.

APPENDIX F
SUPPLEMENTARY DATA

Table E.2 Textural properties and catalytic activity for lactic acid production from glucose

Catalyst	Metal content (mmol/g-cat)	Reaction temperature (°C)	Conversion (%)	Selectivity (%)				
				Lactic acid	Fructose	Glyceraldehyde	Formic acid	Acetic acid
CuCTAB/MgO	1.5	80	32.9	1.4	87.5	-	0.1	0.0
	1.5	100	64.6	3.1	63.9	-	0.3	0.6
	1.5	110	75.1	3.8	35.2	-	0.3	0.7
	1.5	120	100.0	7.0	12.1	1.7	0.6	0.7
	1.5	140	100.0	10.8	0.0	2.4	0.8	0.9
CoCTAB/MgO	1.5	80	26.4	1.4	94.9	-	0.2	0.0
	1.5	100	43.3	2.7	89.9	-	0.3	0.5
	1.5	110	59.7	3.6	49.2	-	0.4	0.7
	1.5	120	100.0	5.8	21.9	1.2	0.4	0.7
	1.5	140	100.0	9.5	0.0	2.0	0.7	0.8

Catalyst	Metal content (mmol/g-cat)	Reaction temperature (°C)	Conversion (%)	Selectivity (%)				
				Lactic acid	Fructose	Glyceraldehyde	Formic acid	Acetic acid
NiCTAB/MgO	1.5	80	40.5	1.6	62.9	-	0.1	0.1
	1.5	100	73.5	4.9	49.4	-	0.2	0.4
	1.5	110	85.8	5.9	26.1	-	0.4	0.6
	1.5	120	100.0	7.9	12.2	1.4	0.4	0.7
	1.5	140	100.0	11.3	0.0	2.7	0.7	0.9
ZnCTAB/MgO	1.5	80	34.8	1.3	79.8	-	0.1	0.0
	1.5	100	70.1	5.2	50.2	-	0.2	0.5
	1.5	110	81.1	6.6	30.6	-	0.2	0.7
	1.5	120	100.0	9.4	14.7	1.3	0.6	0.9
	1.5	140	100.0	12.0	0.0	2.0	0.9	1.0
CuCTAB/MgO	5	110	75.1	6.4	33.9	-	0.8	0.8
CoCTAB/MgO	5	110	70.8	6.0	29.4	-	0.6	0.7
NiCTAB/MgO	5	110	86.5	7.2	30.9	-	0.5	0.7
ZnCTAB/MgO	5	110	82.5	7.9	30.9	-	0.6	0.8

Catalyst	Metal content (mmol/g-cat)	Reaction temperature (°C)	Conversion (%)	Selectivity (%)				
				Lactic acid	Fructose	Glyceraldehyde	Formic acid	Acetic acid
CuCTAB/MgO	10	110	23.2	0.0	29.8	-	0.1	0.0
	10	140	32.7	0.0	55.8	-	0.0	0.0
CoCTAB/MgO	10	110	67.4	4.0	33.7	-	0.6	0.6
	10	140	100.0	10.6	0.0	2.4	0.8	0.7
NiCTAB/MgO	10	110	36.5	0.0	34.2	-	0.2	0.0
	10	140	57.2	0.0	31.0	-	0.0	0.0
ZnCTAB/MgO	10	110	15.5	0.0	51.4	-	0.0	0.0
	10	140	50.9	0.0	32.7	-	0.0	0.0
MgO	-	80	41.5	1.0	46.1	-	0.0	0.0
	-	100	84.9	1.8	28.0	1.7	0.2	0.3
	-	110	89.2	2.6	25.2	2.0	0.4	0.4
	-	120	100.0	5.4	17.6	2.3	0.5	0.7
	-	140	100.0	7.6	0.0	3.7	0.7	1.0

Catalyst	Metal content (mmol/g-cat)	Reaction temperature (°C)	Conversion (%)	Selectivity (%)				
				Lactic acid	Fructose	Glyceraldehyde	Formic acid	Acetic acid
NaOH	-	80	100.0	20.6	0.0	5.5	0.8	0.9
	-	100	100.0	16.9	0.0	3.7	0.8	1.4
	-	110	100.0	14.0	0.0	3.7	0.7	1.6
	-	120	100.0	12.1	0.0	3.7	0.7	1.7
	-	140	100.0	10.3	0.0	3.1	0.7	1.7

VITA

NAME Tanyatorn Udomcharoensab
DATE OF BIRTH 05 December 1993
PLACE OF BIRTH Bangkok
HOME ADDRESS 456/70 Quinn condo, B Building, Ratchada 17, Soi.
Intamara 45, Ratchadaphisek Rd., Bangkok



จุฬาลงกรณ์มหาวิทยาลัย
CHULALONGKORN UNIVERSITY